SuperWASP-N Extra-solar Planet Candidates Between 18hr < RA < 21hr

R.A. Street[1,12,13], D.J. Christian[1], W.I. Clarkson[2,8], A. Collier Cameron[3], B. Enoch[2],
S.R. Kane[3,9], T.A. Lister[3,4,12], R.G. West[7], D.M. Wilson[4], A. Evans[4],
A. Fitzsimmons[1], C.A. Haswell[2], C. Hellier[4], S.T. Hodgkin[5], K. Horne[3],
J. Irwin[5], F.P. Keenan[1], A.J. Norton[2], J. Osborne[7], D.L. Pollacco[1],
R. Ryans[1], I. Skillen[6], P.J. Wheatley[10], and J. Barnes[3,11].

[1]*Astrophysics Research Centre, Department of Physics and Astronomy, Queen's University Belfast, Belfast, BT7 1NN, UK,*
[2]*Department of Physics & Astronomy, The Open University, Milton Keynes, MK7 6AA, UK,*
[3]*School of Physics & Astronomy, University of St. Andrews, North Haugh, St. Andrews, Fife, KY16 9SS, UK,*
[4]*Astrophysics Group, School of Chemistry & Physics, Keele University, Staffordshire, ST5 5BG, UK,*
[5]*Institute of Astronomy, University of Cambridge, Madingley Road, Cambridge, CB3 0HA, UK,*
[6]*Isaac Newton Group of Telescopes, Apartado de correos 321, E-38700 Santa Cruz de la Palma, Tenerife, Spain,*
[7]*Department of Physics & Astronomy, University of Leicester, Leicester, LE1 7RH, UK,*
[8]*Space Telescope Science Institute (STScI), 3700 San Martin Drive, Baltimore, MD 21218, USA,*
[9]*University of Florida, PO Box 112005, 211 Bryant Space Science Center, Gainesville, FL, USA,*
[10]*Dept. of Physics, University of Warwick, Coventry, CV4 7AL, UK.*
[11]*Centre for Astrophysics Research, Science & Technology Research Institute, University of Hertfordshire, Hatfield, AL10 9AB.*
[12]*Las Cumbres Observatory, 6740B Cortona Drive, Goleta, CA 93117, USA.*
[13]*Dept. of Physics, Broida Hall, University of California, Santa Barbara, CA 93106-9530, USA.*

ABSTRACT

The SuperWASP-I instrument observed 6.7 million stars between 8 – 15 mag from La Palma during the 2004 May – September season. Our transit-hunting algorithm selected 11,626 objects from the 184,442 stars within the range RA 18 hr – 21 hr. We describe our thorough selection procedure whereby catalogue information is exploited along with careful study of the SuperWASP data to filter out, as far as possible, transit mimics. We have identified 35 candidates which we recommend for follow-up observations.

Key words: Stars:planetary systems Techniques: photometry

1 INTRODUCTION

The ∼200 exoplanets found to date have revolutionised our understanding of how planetary systems form and evolve (Lin et al. 1996, Burrows et al. 2000). In particular, the discovery of 'hot Jupiters' - Jovian-mass planets in orbits of period⩽5 days where conditions are too hot for them to have formed - led to a reevaluation of the theory of orbital migration (Ipatov 1993, Lin et al. 1996). This class of planets have a comparatively high (∼10%) probability of transiting across the face of their parent star. Transiting exoplanets are highly sought-after as an exceptional range of information can be derived from them; to date 19[1] systems have been discovered. Unambiguous measurements of their physical and orbital parameters can be made, thereby providing quantitative

data against which to test evolutionary models (e.g. Chabrier et al. 2004). Research into the brightest transiting systems has, among other ground-breaking advances, detected components of exoplanetary atmospheres (Charbonneau et al. 2002) and trailing exosphere (Vidal-Madjar et al. 2003, Vidal-Madjar et al. 2004), and placed limits on the existence of moons (Brown et al. 2001) and other planets in the same system (Steffen & Agol 2005). For a comprehensive review of this exciting field, see Charbonneau et al. (2007).

In Section 2 we introduce the SuperWASP project[2] (Pollacco et al. 2006), a wide-angle photometric survey searching for bright transiting planets. Inevitably, all surveys looking for low-amplitude, periodic eclipses will find those caused by stellar as well

---

[1] The Exoplanet Encyclopedia, exoplanet.eu

[2] www.superwasp.org

as planetary objects. Brown (2003) and O'Donovan et al. (2006) discuss several astrophysical systems which can masquerade as transiting exoplanets. The fact that photometric data alone cannot identify transiting planets conclusively was demonstrated by the OGLE project (e.g. Udalski et al. 2004), who have found to date 177 eclipsing candidates, of which 5 have been confirmed as planetary.

We therefore need an effective filtering strategy to eliminate 'false positives' wherever possible in advance of time-consuming follow-up observations. Section 3 describes our system of evaluating candidates to select high-priority objects for follow-up. We discuss the transit candidates discovered within the RA range 18 hr – 21 hr during SW-N's 2004 observing season in Sections 4 – 6.

2   OBSERVATIONS & DATA REDUCTION

SuperWASP-North at the Isaac Newton Group of observatories, La Palma, Canary Islands (hereafter SW-N), is a dedicated ultra-wide field photometric survey instrument observing northern field stars of V∼8–15 mag. Our science goals are designed to explore long baseline (months–years) time domain astronomy, in particular the search for transiting exoplanets. The station supported five cameras in 2004, each with a field of view of $7.8^\circ \times 7.8^\circ$. The instrumentation, observing strategy and data reduction pipeline are described in detail in Pollacco et al. (2006).

The fields monitored were carefully selected to avoid the Galactic plane, in contrast to some other transit surveys. The ecliptic plane was also avoided wherever possible to minimise the sky background due to the Moon and to exclude (Solar System) planets. During the 2004 season we acquired lightcurves for some 6.7 million objects.

A custom-written, fully automated data reduction pipeline, developed by our Consortium, has been applied to the 2004 data (see Pollacco et al. 2006 & Collier Cameron et al. 2006). The photometric output is stored in, and exploited from, the SuperWASP Data Archive held at the University of Leicester. The pipeline routinely achieves a photometric precision of ∼5 millimag for stars with V∼9.5, rising to ∼0.02 mag at V∼13. This gives us a sample of ∼1.2 million stars with which to search for transits from SW-N's first season (see Christian et al. 2006 & Lister et al. 2006).

2.1   RA range 18 hr – 21 hr

The HUNTSMAN algorithm (Collier Cameron et al. 2006) was applied to search for transits in the lightcurves of stars with an RMS of ≲0.02 mag or in practice, those brighter than 13 mag. We note that transits can be detected around late type stars of fainter magnitudes; these will be the subject of a follow-up paper owing to the computational demands of searching much larger numbers of stars. We further constrain our searches to those stars for which we have at least 500 photometric measurements, spanning a period of ⩾10 nights. In total, 184,442 stars met these conditions within the RA range 18 hr – 21 hr, and their distribution is summarised in Table 1.

Our ability to detect transiting planets in these data depends on several factors: the spectral types of monitored stars and the numbers for which we achieve adequately precise photometry, the degree of crowding in the fields, our observing window function and length of the dataset, and not least, the frequency of hot Jovian exoplanets and the distributions of their periods and other physical parameters.

Brown (2003) presents a thorough discussion of the transit recovery rates expected for wide-field transit surveys, emphasising that it is a strong function of planetary period for single-site observations such as ours. He also found that the rate of transit recovery depends on the distribution of spectral types surveyed. Early ground-based surveys (e.g. STARE, Vulcan) concentrated on Galactic Plane fields in order to maximize the numbers of stars monitored. While large numbers of stars are crucial to any such survey, the larger populations of early-type main sequence and giant stars in Galactic Plane fields only serve to exacerbate the blending. These stars do not contribute significantly to the detection statistics since transit amplitude is inversely proportional to the stellar radius, making planetary companions difficult to detect.

For this reason, SW-N has deliberately avoided the crowded Galactic Plane fields, relying instead on our ultra-wide field of view to gather sufficient numbers of stars. Figure 1(a) provides a census of the spectral types covered by our data from a representative field (SW2045+1628), deriving colour information for each star from the 2MASS catalogue. Main sequence stars make up the dominant peak ($J - K < 0.5$) in the SW-N sample. To complement this, Figure 1(b) presents the colour-colour diagram for the same data, extending from ∼late A/early F stars down to approximately early-M type and showing a cluster of points around the solar values of $J - H \sim 0.3$, $H - K \sim 0.1$.

Pont et al. (2006) highlighted the detrimental effect of residual systematic noise in the photometry of this type of survey. While we have gone to great lengths to minimise these systematics (see Section 3.1), the noise in our data is 'red' rather than 'white'. This has the effect of raising the signal-to-noise (S/N) required to detect transiting systems (Smith et al. (2006) investigates the implications for our survey characteristics in detail). In practical terms, an observer must obtain longer baseline data including larger numbers of transits to boost the S/N.

To illustrate this, Figure 2 demonstrates the probability of detecting N_t or more transits as a function of orbital period, P, from the data obtained for several fields illustrating the range of observation intervals spanned in this dataset. A transit is counted as 'observed' if data were obtained within the phase range of $\phi < 0.1\,w/P$ or $\phi > 1 - 0.1w/P$, where w is the expected transit duration, estimated from $w \sim \frac{PR_*}{\pi a}$, where the separation, a is calculated from Kepler's third law. All cases assumed the host star to be a dwarf star of mass $0.9M_\odot$ and radius $R_* = 0.9R_\odot$.

SW produces well-sampled data of acceptable quality most nights and generally ≳40 per cent of a given transit is observed during a detectable event. Setting a detection threshold of only three transits, our data returns 100% of all transiting systems for almost all orbital periods up to ∼5 days. As our observations contain daytime gaps, the probability of identifying systems with periods close to an integer multiples of 1 day or 1.5 days is only ∼35%. The recovery rate also drops for $P \geqslant 4$ days, implying a longer timebase of observations is required. This is particularly noticeable in the SW2045+0928 field, which has the shortest timebase. When the required number of transits is increased to 6, the detectable planets are confined to shorter periods (⩽3 days). Two fields in the RA range, SW2115+0828 & SW2116+1527, have significantly less data than the others: 5 nights in total (spread over >10 nights). They were included in the search automatically as they pass the data criteria, but produced understandably fewer candidates.
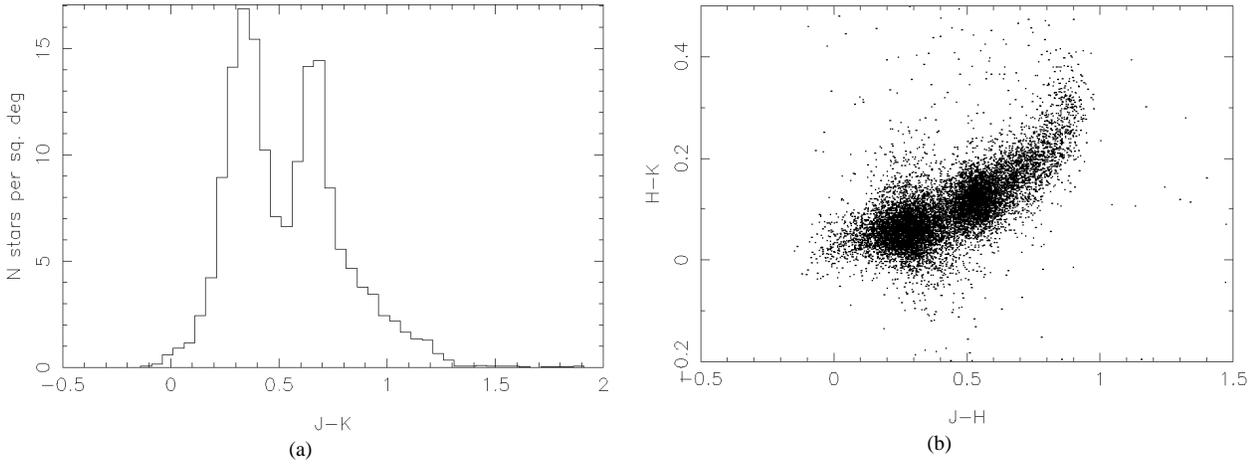
Figure 1. A census of the population of stars monitored in RA=18 hr – 21 hr. The colour information is derived from the 2MASS catalogue.

(a) SW1817+2326 129 nights of data

(b) SW1820+4723 116 nights of data

(c) SW2045+0928 97 nights of data
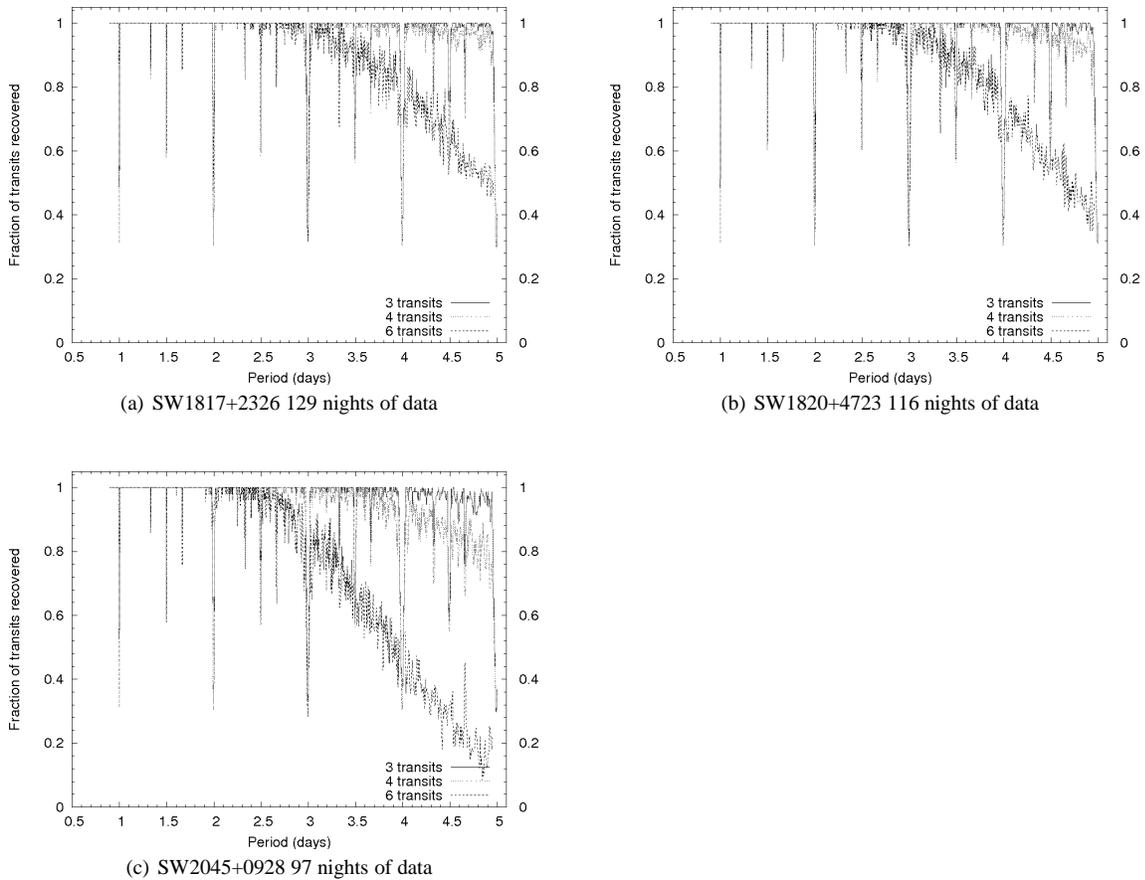
Figure 2. Probabilities of observing more than N_t transits from the 2004 SW-N data for fields within the range RA=18 hr – 21 hr, as a function of the planetary orbital period.

3 THE CANDIDATE SELECTION PROCEDURE

3.1 Stage 1: The HUNTSMAN Transit Finding Package

Collier Cameron et al. (2006) presents a detailed discussion of the corrections applied to the SW-N photometry and the nature of the adapted-Box-fitting Least Squares transit-hunting algorithm em-

ployed here. It produces a 'periodogram' of the difference in the goodness-of-fit statistic $\Delta\chi^2$ between each model relative to the no-transit case, plotted against transit frequency.

HUNTSMAN rejects obviously variable stars with $\chi^2 > 3.5N$ (N=number of datapoints), those less than 2 transits, and those solutions which have phase gaps in the folded lightcurve greater

Table 1. J2000.0 coordinates of field centres surveyed in this work, giving for each field the number of targets searched by the transit-hunting algorithm, and the number of stars selected by it.

RA	Dec	No. nights	No. targets	No. stars extracted	DAS
18 16 00	+31 26 00	127	19,810	1396	3
18 17 00	+23 26 00	129	24,220	1737	4
18 20 00	+39 23 00	118	16,429	850	4
18 20 00	+47 23 00	116	14,085	1011	3
20 45 00	+09 28 00	97	21,390	1090	1
20 45 00	+16 28 00	5	2,259	90	1
20 45 00	+16 28 00	116	25,971	1226	2
20 46 00	+24 45 00	104	26,873	1669	5
21 14 00	+16 28 00	116	17,747	1220	3
21 15 00	+08 28 00	116	14,225	1200	4
21 15 00	+23 51 00	5	689	55	3
21 16 00	+15 27 00	5	744	82	4
Total			184,442	11,626	

than $2.5\times$ the transit duration. A candidate's signal-to-red noise ratio, S_{red}, must be greater than 5.0, taking account of the dominance of systematics in the photometric noise (Pont et al. 2006). The strongest peaks in the $\Delta\chi^2$ periodogram corresponding to brightening and dimming are used to define the "anti-transit ratio" (Burke et al. 2006), $\Delta\chi^2/\Delta\chi^2_-$. Candidates must have $\Delta\chi^2/\Delta\chi^2_->1.5$. The algorithm also estimates the degree of ellipsoidal variation in the out-of-transit lightcurve by producing a signal-to-noise statistic, S/N_{ellip}.

HUNTSMAN selected 11,626 candidates in total from the fields in this dataset, summarised in Table 1. In the next section we describe the subsequent stages of systematic candidate assessment employed to eliminate interlopers.

3.2 Stage 2: Visual Assessment of Lightcurves

A visual inspection was made of each lightcurve in conjunction with the corresponding periodogram of $\Delta\chi^2$ plotted against frequency. For a candidate to be selected, it had to display a clear transit with credible amplitude, width and period and a smoothly sampled folded lightcurve. Our finite-length, single-site observations meant that lightcurves folded on multiples of 1 day were by far the most common transit mimic. The vast majority of these cases were rapidly eliminated on sight as they showed no clear transit signal. Many classes of obvious stellar binaries or variables were also removed from the candidate list.

We developed the following 4-digit coding scheme to try to quantify this subjective inspection process as far as possible.

- Digit 1: Shape and visibility of the transit.

1 Clear transit-shaped signal of credible width and depth.
2 Shallow/noisy but clearly visible transit signal.
3 Transit barely visible, either very shallow, lost in noise or ill-shaped.
4 Partial transit or gaps around phase 0 but still showing clear transit morphology.
5 Signs of a dip at phase 0 but no clear in/egress.

- Digit 2: Out-of-transit lightcurve.

1 Clean and flat, no other variations.
2 Noisy but flat.

3 Signs of ellipsoidal variation or suspected secondary eclipses (includes some candidates which have been folded on twice the period).
4 Shows low-amplitude sinusoidal variation on short timescales, giving a 'knotty' appearance (can indicate that the lightcurve is folded on the wrong period).
5 Realistic variability of some other form out of transit.
6 Multi-level or 'jumpy' lightcurves (can indicate the wrong period or photometry artifacts).

- Digit 3: Distribution of points in the folded lightcurve.

1 Smoothly sampled with a similar density of points throughout.
2 Some minor regions with slightly lower density of points, retaining a clear signal.
3 Significant clumpy of data points (can indicate a pathological period).

- Digit 4: Credibility of determined period.

1 No reason to doubt measured period, clear peak in $\Delta\chi^2$ periodogram.
2 Period gives a secure signal visible in the folded lightcurve, but peak lies close to a known alias. Sometimes associated with gaps in the folded lightcurve.
3 Signal visible in folded lightcurve but period is a known alias or peak lies at a commonly-occurring frequency.
4 Lightcurve suggests that the measured period is wrong.

We emphasize that this is designed to guide the manual selection of targets, rather than to provide a hard 'statistic' on which a threshold cut might be applied. The code for each star was assessed on a case-by-case basis. That said, stars coded '[4,5]nnn', 'n[5,6]nn', or 'nn[3]n' were almost always eliminated unless there were very clear signs of a planet-like transit within the lightcurve despite its shortcomings. Candidates with '[3]nnn' or 'n[3,4]nn' were assessed with caution. However, targets with 'n[3]nn' and/or 'nnn[4]' that otherwise showed a clear transit signal were retained and alternative periods were explored.

This process uncovered several exciting, high S/N planetary candidates but inevitably also produced a number of cases close to the threshold. Like all our candidates, such cases were required to have believable transit-like lightcurves and credible parameters sufficient to pass our criteria. Nevertheless, some stars, while in-

triguing, only just made the cut. For instance, some objects demonstrated a clear, transit-like lightcurve, but had a period close to an integer multiple of 1 day. Others were close to the cut-off for ellipsoidal variation. Since objects in this category were potentially low-mass-star or brown dwarf binaries and therefore of independent interest, they were retained in the candidate list but not shortlisted after Stage 4.

3.3 Stage 3: Selection Criteria

Surviving candidates were subject to the following requirements:

- The S_{red} must be at least 8.0.
- The period must be $\geqslant$ 1.05 days. This criterion is implemented in order to reject candidates folded on one-day aliases.
- The number of transits observed must be $\geqslant$ 3.
- Anti-transit ratio must be greater than 2.0.
- The S/N_{ellip} should be less than about 8.0. While this threshold was generally reliable, a number of objects were found which had a value of S/N_{ellip} exceeding this threshold yet the out-of-transit lightcurve appeared flat to visual inspection. In cases with exceptionally clear, believable transit-like lightcurves, a degree of human discretion was afforded.

We elected not to search for transits with periods less than 1.05 d as early test runs resulted in unfeasibly large numbers of false alarms folded on periods that are integer fractions of 1 d. It was decided that separate searches would be run for very short (and long) period planets after the present work had cultivated experience in false-positive rejection.

3.4 Stage 4: Compilation of Catalogue Data

Objects surviving this cull were submitted to SW's online *Variable Star Investigator* tool (Wilson et al. 2007), which performs automated queries on a number of existing photometric catalogues including 2MASS (Skrutskie et al. 2006), Tycho-2 (Høg et al. 2000), Simbad (Wenger et al. 2000) and Hipparcos (Perryman et al. 1997) among others. This provided for each candidate a table of multi-colour photometric information, lists of other nearby objects falling within SW-N's photometric aperture of $\sim 48''$ and $3' \times 3'$ and finderchart from DSS (Cabanela et al. 2003) and 2MASS. The latter information was used to assess the degree to which each star is blended in the SW-N photometry, a major cause of false positives. If a brighter object was found within a candidate's aperture, then that star was removed from the target list.

Two separate temperature-colour relationships were employed to estimate the temperature of each candidate star, assuming it to be main sequence and that the measured colours were not contaminated by light from the companion (as expected under the exoplanet hypothesis). The first relationship uses Tycho-2 V_T and 2MASS K with an uncertainty of 91K and the second, 2MASS J & H (uncertainty 186K):

$$T_{eff} = 213.19(V_T - K)^2 - 1920.1(V_T - K) + 8335.7, \quad (1)$$
$$T_{eff} = -4369.5(J - H) + 7188.2, \quad (2)$$

These were derived from the temperature data on 30,000 FGK dwarf stars presented in Ammons et al. (2006) for which the precision of the Tycho-2 and 2MASS photometry is better than 1%. The use of the second relation, based on infrared colours, is more sensitive to the presence of cooler companion bodies. A significant discrepancy between the two temperature (and hence radius) estimates can therefore indicate the presence of a companion (often stellar).

The colour indices, together with the USNO-B1.0 proper motions (μ) were also used as an indicator of the luminosity class of the target. The Reduced Proper Motion (RPM_J) was computed from:

$$RPM_J = J + 5\log_{10}\mu. \quad (3)$$

Plotted against the $J - H$ index, dwarfs are separated from giants, as they lean towards higher values of RPM_J and low $J - H$. A polynomial boundary was set between the two groups so that *VSI* could issue a warning when this threshold is crossed. Brown (2003) demonstrated that $J - K$ colours can also act as a rough indicator of luminosity based on data from the STARE project. Taking this and Charbonneau et al. (2004) as a guide, *VSI* flags any star with a $J - K > 0.7$ as a possible giant.

The derived T_{eff} values were then used to estimate the spectral type of the host star based on data from Cox (2000) while the radius and mass were estimated using data from Gray (1992). For $T_{eff} < 7000$ K, the RMS of the fit of polynomial functions describing T_{eff} .vs. radius and mass were 0.016 K in both cases.

A minimum limit on the radius of the companion, R_p, was estimated from the stellar radius, R_* and the transit amplitude, δ, using the relationship derived by Tingley & Sackett (2005) for the I-band:

$$R_c \approx \sqrt{\frac{\delta}{1.3}R_*^2}, \quad (4)$$

Our unfiltered, wide bandpass photometry is dominated by the red sensitivity of the CCD and the uncertainty introduced by approximating to I-band is smaller than that of the stellar radius estimate.

Although electron degeneracy means that there can be little difference in the radii of objects between $0.5 M_\odot - \sim 1 M_{Jup}$, we concentrated on objects with predicted R_p of less than $\sim 2 R_{Jup}$. To aid selection, we also employed the η_p diagnostic derived by Tingley & Sackett (2005), comparing the observed transit duration D_{obs} with that theoretically predicted (D_{pred}) for a transiting hot Jupiter:

$$\eta_p = \frac{D_{obs}}{D_{pred}} \quad (5)$$
$$= \frac{D_{obs}}{2Z(1+\sqrt{1.3/\delta})}\left(\frac{2\pi GM_\odot}{P}\right)^{\frac{1}{3}} R_c^{-\frac{7}{12}} R_\odot^{-\frac{5}{12}} \left(\frac{1.3}{\delta}\right)^{\frac{5}{24}} \quad (6)$$

where Z is a factor representing the effects of the projected orbital inclination, set equal to 1 (see discussion in Tingley & Sackett 2005), δ is the depth of the transit and P is the period. Strong exoplanet candidates are expected to have $\eta_p \sim 1$. However, caution was exercised when using this criterion to judge our candidates since the value of R_p depends heavily on the value of R_*, the estimate of which is subject to significant uncertainty when made from colour indices alone.

Our assessment of characteristics was quantified using three additional indices from the following coding scheme.

- Planetary radius, R_p.
A. $R_p < 1.6\,R_{Jup}$.
B. $1.6 \leqslant R_p \leqslant 1.75\,R_{Jup}$.
C. $R_p \geqslant 1.75\,R_{Jup}$.

- Exoplanet diagnostic η_p.
A. $0.5 \geqslant \eta_p \geqslant 1.5$.
B. $\eta_p < 0.5$.
C. $\eta_p \geqslant 1.5$.

- Blending.
A. No other objects within aperture.
B. 1 or 2 other objects less than 5 mags fainter than target within aperture.
C. More than 2 objects less than 5 mags fainter than target within aperture.
D. Brighter objects within the aperture.

Each candidate was then assessed in turn, taking into account all available data, and a final shortlist of high-priority candidates was produced. In the next section we summarise the results for stars in the RA range 18 hr - 21 hr.

It can be seen from this discussion that some selection cuts are repeated during subsequent stages using increasingly stringent thresholds. For instance, HUNTSMAN executes an automatic cut of objects with $S_{red} < 5.0$, while at Stage 3, a further cut is made at $S_{red} < 8.0$. In exploring the first large-scale transit hunting results from SW, we took a cautious approach in order to investigate the most effective selection criteria. Not wanting the algorithm to dismiss interesting objects before human interpretation, the initial thresholds were set low, systematically rising for successive stages of evaluation. Needless to say, lessons learned from this season's work will enable us to streamline the procedure in future.

4 RESULTS

The HUNTSMAN algorithm flagged 11,626 objects for attention. Stage 2 visual inspection concluded that 775 of these were of genuine interest. The Stage 3 selection requirements detailed in Section 3.3 sifted this list down to 77 stars, the details of which are presented in Table 2.

The visual lightcurve assessment of each star is quantified by a 4-digit code in column 11. At this stage, the list contained 19 borderline candidates, many of which are likely low-mass binaries. As these objects are of independent interest, we have included their full parameters in Tables 2 & 3, marked by †, although these objects were not carried through to the final shortlisting as the present paper deals with planetary candidates only.

The remaining 58 objects surviving to Stage 4 could be grouped into three broad classes. Twenty-four stars received the best grades (between '1111' and '2222'), indicating a clear, credible transit signal in a flat, well sampled lightcurve. Seventeen objects were flagged as displaying a credible transit signal, but on a period not correctly identified. A further 17 candidates were found to show plausible transits signals and were only downgraded on the grounds of low S/N.

At this stage we attempted to eliminate astrophysical false positives by considering the catalogue information available, estimating the companion radius and corresponding value of η_p and assessing the degree of blending in the field.

Table 3 gives the full set of parameters for these candidates. Each candidate was then evaluated on its merits, including a visual examination of both folded and unfolded lightcurves. Where relevant, target lightcurves were re-folded on the periods of the alternative peaks from the periodogram. In a small number of cases, this showed that the true period fell outside HUNTSMAN's search range of 0.9 – 5 days. We then applied the algorithm developed by Schwarzenberg-Czerny (1989),Schwarzenberg-Czerny (1999) (referred to as S-C) to determine the correct period.

Evaluating all the information available for all candidates highlighted 35 objects of particular interest at the stage 4; the remaining objects being rejected as likely stellar binaries, some blended. These are printed in bold in Tables 2 & 3 and their folded lightcurves and $\Delta\chi^2$ periodograms are presented in Figures 3–7. We discuss these objects individually below, and indicate particularly strong planetary candidates. However, all of these objects deserve follow-up observations as 'false alarms' from a transit survey include interesting low-mass binaries.

4.0.1 1SWASP J181317.03+305356.0

This object displayed a distinct, if noisy, dip when folded on its original period of 4.499 days but this resulted in gaps in the phase coverage. The transit is still visible when the data is folded on a period of 2.248 days but this time the lightcurve is more smoothly sampled and flat out of transit to visual inspection. The new parameters imply a Jovian-sized companion object (R_p=1.05 R_{Jup}) supported by a reasonable η_p=0.71, but while the target is the brightest object in its field it has sufficient nearby faint stars for blending to be a possibility. More observations are required for this object.

4.0.2 1SWASP J181454.99+391146.0

The faintness of this object (12.796 mag) accounts for the degree of noise in the lightcurve, but the transit is still visible. The noise makes it difficult to judge the flatness out of transit, though the S/N_{ellip} is 0.659. The period is close to the 1-day alias at 1.10 days, but this is derived from a clear strong peak in $\Delta\chi^2$. Otherwise, the amplitude and the transit duration are reasonable, supported by an η_p=0.92. The primary star appears to be late type, implying a relatively small companion (0.89R_{Jup}). However, this object lies in a fairly crowded field, so it may be a blended stellar binary.

4.0.3 1SWASP J181958.25+492329.9

The brightness of this 10.6 mag object allows us to detect transits only $\sim$6 mmag deep in this flat lightcurve. The period was confirmed independently with the S-C algorithm and transit signatures identified by visual inspection of the unfolded lightcurve. The host star has a solar spectral type so the estimated companion radius is very low: 0.69R_{Jup}, supported by an η_p close to 1. This makes it an exciting candidate for follow-up despite the serious crowding in this field. However, further observations are required to eliminate the possibility of a blended eclipsing binary.

4.0.4 1SWASP J182620.36+475902.8

The folded lightcurve clearly shows a fairly deep, wide, 'V'-shaped dip (which might indicate a stellar binary) but no obvious ellipsoidal variations. The period is 3.04 days, close to a multiple of the 1-day alias, but the signal is clear with a credible number of transits observed. The object is unblended and has an estimated companion radius of 1.6R_{Jup}; however the η_p of 1.49 would support the stellar binary hypothesis.

Table 2. Initial list of candidates after Stage 3. Borderline candidates are marked with † and are listed for information.

Identifier 1SWASP...	V_{SW} (mag)	Period (days)	Duration (hrs)	δ (mag)	N_{tr}	S_{red}	$\Delta\chi^2$	S/N_{ellip}	$\Delta\chi^2/\Delta\chi^2_-$	Code
†J175919.79+353935.1	11.824	4.846186	4.272	0.026	6	9.264	338.197	0.605	5.327	2223
†J180103.13+511557.1	9.988	4.785081	3.672	0.0145	8	11.215	928.888	2.401	3.467	2423
J180304.96+264805.4	11.782	2.364723	5.136	0.0254	20	13.453	1454.973	4.145	9.616	3211
J180726.64+224227.9	12.568	2.121623	5.256	0.0173	21	9.548	375.908	4.150	3.302	3314
†J181129.19+235412.4	12.884	4.234895	8.568	0.0578	16	11.584	2580.622	1.699	9.145	1314
J181317.03+305356.0	**12.046**	**4.498677**	**1.92**	**0.0194**	**13**	**14.446**	**540.914**	**4.992**	**6.704**	**1134**
J181454.99+391146.0	**12.796**	**1.102625**	**1.56**	**0.0235**	**25**	**13.297**	**219.564**	**0.659**	**5.134**	**1212**
J181958.25+492329.9	**10.6**	**2.368548**	**2.424**	**0.0061**	**16**	**10.759**	**145.924**	**0.241**	**2.902**	**3111**
J182127.09+200011.7	11.449	2.647752	4.248	0.0366	18	16.824	2831.871	2.789	15.396	1111
J182131.07+483735.5	12.164	1.809191	2.832	0.0167	16	9.781	470.931	2.314	4.140	3211
J182333.22+222801.2	12.788	1.821008	3.432	0.0421	18	17.315	983.6475	8.064	12.2324	1211
†J182339.64+210805.5	12.794	1.585846	2.088	0.0245	22	10.374	306.613	6.991	2.312	1314
J182346.12+434241.3	11.771	2.969366	3.384	0.0295	11	19.982	444.963	0.895	11.656	1124
J182620.36+475902.8	**11.584**	**3.04365**	**4.032**	**0.0628**	**13**	**24.415**	**10754.299**	**4.225**	**11.474**	**1112**
†J182626.38+374954.8	11.614	4.698312	4.944	0.0157	8	13.104	317.828	1.643	6.417	2213
J182916.00+235724.8	12.043	4.465326	1.752	0.0373	7	12.356	578.442	3.163	11.565	2224
J182924.67+232200.2	**11.331**	**3.678186**	**2.952**	**0.0173**	**10**	**14.248**	**244.980**	**2.174**	**2.639**	**3123**
†J182927.04+233217.1	10.8	4.903747	4.704	0.0063	9	8.214	146.459	1.954	2.299	3214
†J183043.97+230526.1	9.31	3.680977	4.296	0.0098	9	11.139	628.645	3.278	4.027	2311
J183104.01+323942.7	**11.027**	**2.378781**	**1.776**	**0.0089**	**15**	**11.013**	**256.230**	**2.065**	**4.873**	**2111**
J183104.12+243739.3	12.789	1.492383	1.92	0.0197	20	10.218	188.009	4.411	2.836	1314
J183431.62+353941.4	**10.485**	**1.846796**	**2.28**	**0.0127**	**17**	**12.111**	**787.959**	**0.691**	**3.635**	**1111**
†J183517.51+390316.2	9.823	4.073428	5.16	0.012	8	9.282	1320.766	5.377	2.225	1123
J183723.62+373721.9	11.851	3.300887	4.32	0.0251	13	13.599	841.3629	8.779	10.1919	1213
J183805.57+423432.3	**12.641**	**3.515957**	**4.104**	**0.0197**	**9**	**8.815**	**127.097**	**0.999**	**3.693**	**3131**
J184119.02+403008.4	**12.157**	**3.734014**	**4.224**	**0.0148**	**11**	**9.449**	**198.451**	**0.502**	**2.720**	**3133**
J184303.62+462656.4	**11.935**	**3.338103**	**4.08**	**0.0265**	**11**	**12.248**	**1065.843**	**1.867**	**9.098**	**4124**
J202820.25+094651.0	11.108	2.146933	4.776	0.0085	16	12.533	294.491	3.910	5.344	2111
J202824.02+192310.2	**12.16**	**1.257835**	**2.424**	**0.0222**	**23**	**13.111**	**589.550**	**3.355**	**7.095**	**1111**
†J202907.09+171631.7	12.786	4.117398	4.968	0.0309	11	9.996	450.143	1.126	3.844	2223
J203054.12+062546.4	**11.98**	**2.152102**	**1.296**	**0.0168**	**11**	**9.463**	**217.184**	**5.522**	**3.262**	**1111**
†J203229.10+132820.9	12.471	4.632829	4.608	0.047	9	12.773	1385.902	2.670	11.318	2213
J203247.55+182805.3	12.157	2.522688	7.776	0.0118	22	11.579	308.408	0.875	5.324	3113
J203314.77+092823.4	**11.78**	**1.753056**	**3.048**	**0.0316**	**18**	**14.221**	**2154.619**	**7.012**	**8.927**	**1111**
J203315.84+092854.2	**11.943**	**1.752371**	**2.784**	**0.0413**	**16**	**13.545**	**2796.5991**	**9.663**	**11.4699**	**1211**
J203543.98+072641.1	10.094	1.85463	2.76	0.0195	13	16.884	3354.689	1.083	10.542	1112
J203704.92+191525.1	**11.301**	**1.68011**	**1.416**	**0.0095**	**16**	**9.344**	**245.231**	**3.226**	**2.826**	**3111**
J203717.02+114253.5	11.327	3.118049	2.496	0.0274	8	12.11	2792.375	3.870	21.267	1111
J203906.39+171345.9	**9.716**	**1.348858**	**1.968**	**0.0173**	**18**	**17.059**	**2934.2539**	**8.365**	**47.1445**	**1124**
†J203932.30+162451.1	10.904	1.520504	8.976	0.02	39	14.359	10012.064	0.966	2.936	2311
J204125.28+163911.8	**11.243**	**1.221506**	**2.88**	**0.008**	**28**	**11.48**	**518.131**	**2.703**	**3.151**	**3111**

4.0.5 1SWASP J182924.67+232200.2

We handle this object with caution because the transit signature is unclear for the partially owing to its period (3.68 days) and also to the intrinsic scatter in the lightcurve. Nevertheless, transit-like dips were identified from visual inspection of the unfolded lightcurve. No other variability is evident. The companion radius is credible for a planet at $1.26R_{Jup}$ supported by η_p=0.88. This star is significantly brighter than any other object within $\sim3'$ although blending cannot be ruled out. We recommend obtaining more data on this object, to confirm the transit-like signal.

4.0.6 1SWASP J183104.01+323942.7

The low amplitude (0.0089 mag) and short duration (1.8 hrs) of this event would have made it difficult to detect in a fainter star. Our lightcurve shows little out-of-transit variation and a clear, credible period. The predicted radius of $0.97R_{Jup}$ is supported by a slightly low but acceptable value of η_p=0.61. As this candidate lies in an uncrowded field it is a strong planetary candidate.

4.0.7 1SWASP J183431.62+353941.4

The classic, flat-bottomed transit signature is clear in the folded lightcurve of this bright (10.5 mag) star, which shows no other signs of variability and a reasonable if quite short period. The companion radius of $1.3R_{Jup}$ is within the expected range for a hot Jupiter, and an η_p of 0.78 makes it believable. The high degree of blending around this candidate raises a warning flag for an otherwise strong candidate.

4.0.8 1SWASP J183805.57+423432.3

This folded lightcurve shows a degree of clumping because the period of ~3.5 days requires a longer timebase of observations to

Table 2 – *continued* Initial list of candidates after Stage 3. Borderline candidates are marked with † and are listed for information. Parenthesis around an object indicates that spectroscopic data are discussed in Section 5.

Identifier 1SWASP...	V_{SW} (mag)	Period (days)	Duration (hrs)	δ (mag)	N_{tr}	S_{red}	$\Delta\chi^2$	S/N_{ellip}	$\Delta\chi^2/\Delta\chi^2_-$	Code
†J204142.31+052007.5	12.422	3.216912	4.776	0.0279	8	10.462	317.078	0.533	7.574	2232
J204142.49+075051.5	**12.082**	**1.381342**	**1.968**	**0.0096**	**19**	**11.739**	**165.756**	**1.413**	**7.403**	**3114**
J204211.19+240145.1	11.588	1.792911	2.424	0.0518	10	14.079	1074.758	6.535	2.917	4134
J204323.83+263818.7	**11.561**	**1.419959**	**1.2**	**0.0369**	**10**	**18.496**	**179.712**	**0.971**	**2.440**	**1224**
†J204328.95+054823.1	12.616	3.939179	2.328	0.0617	10	16.96	1989.211	5.293	17.029	1322
(J204456.57+182136.0	12.596	2.71611	4.584	0.0202	16	12.164	525.040	1.287	14.612	3214)
J204617.02+085412.0	**12.28**	**1.947141**	**2.184**	**0.0095**	**14**	**9.436**	**92.943**	**0.647**	**2.163**	**3112**
J204712.42+202544.5	**12.386**	**2.61264**	**2.064**	**0.0275**	**10**	**13.103**	**355.276**	**3.327**	**6.693**	**2211**
J204745.08+103347.9	**11.648**	**3.235407**	**3.648**	**0.0289**	**8**	**16.376**	**1336.114**	**5.186**	**16.348**	**1112**
†J204905.55+110000.4	12.891	1.371571	1.584	0.023	20	12.8	244.376	4.343	4.619	1311
J205027.33+064022.9	**10.164**	**1.229345**	**3.192**	**0.0096**	**20**	**13.641**	**1198.006**	**6.691**	**5.830**	**3111**
†J205218.75+182330.0	11.991	2.197814	3.48	0.0441	16	19.038	3378.642	3.256	22.912	1131
J205223.03+151046.8	11.493	1.454887	2.4	0.0301	23	19.47	3389.000	2.060	21.470	1114
J205302.40+201748.3	10.853	4.931719	8.88	0.0084	9	8.327	360.930	0.093	2.553	3123
J205308.03+192152.7	**11.13**	**1.676449**	**2.736**	**0.0068**	**23**	**10.406**	**213.332**	**0.668**	**3.508**	**2111**
J205438.05+105040.7	11.428	2.623442	2.664	0.0405	11	16.117	3278.368	4.645	8.251	1114
J210009.75+193107.1	**10.422**	**3.054875**	**2.424**	**0.0082**	**9**	**8.877**	**303.455**	**1.646**	**2.612**	**3113**
†J210130.24+190021.7	12.14	2.683587	1.584	0.0697	12	23.253	1860.082	5.557	31.460	1311
J210151.43+072326.7	**12.476**	**2.220785**	**2.472**	**0.0138**	**15**	**8.764**	**108.956**	**0.948**	**2.396**	**3213**
†J210231.79+101014.5	12.635	1.506187	1.608	0.0296	16	14.97	258.766	6.760	2.971	1332
J210318.01+080117.8	**11.909**	**1.223824**	**1.92**	**0.0167**	**24**	**12.784**	**466.284**	**0.248**	**4.999**	**1111**
†J210335.82+125637.6	12.387	1.447543	2.856	0.0146	24	9.082	268.208	1.208	4.420	2213
J210352.56+083258.9	**11.636**	**3.89368**	**3.504**	**0.0227**	**11**	**13.38**	**953.011**	**7.066**	**11.909**	**1112**
J210909.05+184950.9	**9.912**	**2.91879**	**2.664**	**0.0083**	**13**	**9.718**	**801.126**	**0.121**	**3.041**	**3112**
J210912.02+073843.3	**11.262**	**1.36983**	**2.28**	**0.0213**	**22**	**16.035**	**1594.4681**	**12.508**	**20.6406**	**1111**
J211127.41+182653.3	12.291	4.216933	3.168	0.0464	8	20.186	1043.324	0.775	25.743	2211
J211417.15+112741.0	11.246	2.519934	2.784	0.0336	11	10.555	2902.904	1.290	3.334	3214
J211448.98+203557.1	12.453	4.864666	4.632	0.0525	8	13.794	1939.578	4.542	16.558	1212
J211608.42+163220.3	**11.308**	**3.468244**	**1.992**	**0.0131**	**10**	**13.461**	**228.680**	**0.781**	**5.584**	**1111**
J211645.22+192136.8	**9.432**	**1.466001**	**1.68**	**0.012**	**16**	**12.273**	**1379.556**	**2.033**	**3.516**	**2124**
J211817.92+182659.9	12.395	4.419854	3.36	0.0274	9	12.149	716.481	1.194	9.733	3214
J212532.55+082904.4	**11.343**	**3.125014**	**2.688**	**0.0267**	**9**	**14.313**	**1013.935**	**1.980**	**7.591**	**1212**
J212749.35+190246.0	12.317	4.870738	3.408	0.0438	10	10.158	1332.879	1.191	2.215	2224
†J212815.28+082933.7	10.165	4.91815	5.592	0.0083	9	8.493	374.959	0.644	2.249	3414
J212843.62+160806.2	**11.453**	**1.375647**	**2.64**	**0.0159**	**25**	**15.572**	**1288.665**	**8.841**	**9.5499**	**1111**
J212855.03+075753.5	**12.241**	**4.688048**	**1.92**	**0.0297**	**5**	**9.54**	**188.137**	**0.953**	**2.503**	**3213**

cover the full phase range. Dips are clearly visible in the unfolded data although the $V \sim 12.6$ mag means there is a high degree of intrinsic scatter in the data. However, the star lies in a relatively uncrowded field and the nearest companions are $\gtrsim 10$ arcmins away. The late-type host star leads us to infer a small companion radius of $0.86 R_{Jup}$. Although this is tempered by an η_p of 1.6, this object remains a candidate.

4.0.9 1SWASP J184119.02+403008.4

The transit signature in this folded lightcurve is unclear for the same reasons given for 1SWASP J183805.57+423432.3. As above, the validity of the measured signal was confirmed by visual inspection of the unfolded data. No other variation is evident in the lightcurve. The predicted companion radius of $0.92 R_{Jup}$ is tempered by a slightly elevated $\eta_p=1.45$, but is the brightest object in an uncrowded field.

4.0.10 1SWASP J184303.62+462656.4

The original lightcurve showed a 'V'-shaped dip at phase 0.0 with additional points around phase -0.45, which gave the appearance that the correct period was not identified. The gaps in the lightcurve indicate that the true period lies close to an alias making it difficult to determine. This is supported by investigation with the S-C algorithm, which suggested a period around 10 days; the lightcurve in Figure 4(b) is shown folded on the strongest peak found by HUNTS-MAN. The predicted companion radius given these parameters is only $1.25 R_{Jup}$, although the eclipse durations are longer than those expected for a planetary transit ($\eta_p=1.86$). This object could be a low-mass binary and although it suffers from blending, we recommend that it continue to be observed.

4.0.11 1SWASP J202824.02+192310.2

This object displays transits of credible width and depth in an otherwise flat, if noisy, lightcurve. The host star colour implies a radius of $1.29 R_\odot$ and a fairly large companion object at $1.64 R_{Jup}$ ($\eta_p=0.94$). However, light from a number of nearby stars

will have contaminated the photometry, so this could be a stellar binary.

4.0.12 1SWASP J203054.12+062546.4

The data for this target show a brief but quite well defined signal in an otherwise flat, if noisy, lightcurve. The period and amplitude are believable for a planetary companion of $0.83R_{Jup}$ with a low but acceptable η_p of 0.59. The few nearby objects raise the possibility of contaminating light but this remains a candidate.

4.0.13 1SWASP J203314.77+092823.4 & J203315.84+092854.2

These objects both display a similar periodicity at $P\sim1.75$ days and are blended. It should be noted that J203315.84+092854.2 was actually eliminated at Stage 3 since it has $S/N_{ellip} = 9.663$. This object was only retained because J203314.77+092823.4 passed the automatic criteria, but could not be considered in isolation. Both lightcurves are a little noisy and the transit has quite shallow in/egress slopes, but no other activity is apparent. The late spectral type of the former star makes this system interesting, implying a $0.94R_{Jup}$ companion radius but the $\eta_p=1.59$ suggest the observed dips are longer than expected for a planetary object. The eclipses are more likely to be due to the latter object, an F2-F5 type, with a companion of radius $2.53R_{Jup}$ ($\eta=0.87$).

4.0.14 1SWASP J203704.92+191525.1

The very low amplitude (9.5 mmag) and short (1.4 hr) duration of this candidate makes the transit dips difficult to detect, but the signal is seen in the unfolded lightcurve and S-C periodogram. Obtaining follow-up photometry with a large telescope is therefore recommended. The predicted companion radius is close to that of Jupiter but the value of η_p is quite low, 0.55, implying that the observed transit duration is short compared with theoretical predictions. The target does have 2 other stars nearby so blending is a consideration.

4.0.15 1SWASP J203906.39+171345.9

Datapoints overlapping the clear transit-like dip indicated that the true period for this object was twice that found by HUNTER, i.e. 2.697 days. The 'V'-shape morphology then becomes clear in a flat, if noisy, lightcurve, and the predicted planet radius is only $1.35R_{Jup}$ with $\eta_p=0.79$. This object is the brightest in a crowded field, and suffers from significant blending.

4.0.16 1SWASP J204125.28+163911.8

Despite the low amplitude of this candidate, visual inspection of the unfolded data confirms the occurrences of transit-like dips, and the S-C algorithm produces a strong spike at a frequency of $1/1.221$ days. The predicted companion radius is extraordinarily low at $0.53R_{Jup}$ owing to the very red colour of the host star, which is classified as a mid-K type. The high value of η_p though, warns that the eclipse duration is longer than expected, and the star, while by far the brightest object in its field, does have nearby companions. Overall, we recommend this object for further investigation.

4.0.17 1SWASP J204142.49+075051.5

The low amplitude (10.2 mmags) and faint magnitude ($V\sim12$ mag) of this object conspire to produce a very shallow transits of ~2.3 hrs duration. Their existence was confirmed by visual inspection however, and the strongest peak in the S-C periodogram corresponds to 2.763 days. Once folded on this period, the lightcurve shows no other form of variation from the mid- to late-K type host star. The low predicted companion radius, $0.59R_{Jup}$, makes this an exciting candidate, particularly in the light of the $\eta_p=1.04$. Some nearby stars raise a caution of potential blending.

4.0.18 1SWASP J204323.83+263818.7

This star displays a clear 'V'-shaped dip when the lightcurve is folded on the period of one of the top five peaks, $P=1.421$ days. Transits were observed of reasonable amplitude (0.04 mag) and fairly short (1.32 hr) duration, however there are hints of ellipsoidal variation and faint signs of secondary eclipses. The estimate radius for the companion object is a promising $1.32R_{Jup}$, though with a comparatively low $\eta_p=0.63$, but this star has a very close companion and is certainly affected by blending. High resolution imaging and/or spectroscopic observations are required to confirm or dismiss this candidate.

4.0.19 1SWASP J204617.02+085412.0

Another case where faint magnitude ($V\sim12.3$ mag) and low amplitude (9.5 mmag) mask the transit signal, but close inspection reveals a series of shallow dips. The S-C periodogram is unclear, the period being so close to 2 days, but the folded lightcurve shows a transit-like dip in an otherwise flat dataset. The G-type host star has one very close blended star, albeit a much fainter one as well as a group of other stars within the aperture, meaning the true companion radius could well be greater than the predicted $0.91R_{Jup}$. Nevertheless, we recommend this object for follow-up observations.

4.0.20 1SWASP J204712.42+202544.5

The faintness of this star (12.386 mag) leads to a noisy but apparently flat lightcurve except for a clear and credible transit dip. The host star's IR colour suggests a mid-K spectral type and a companion radius of $0.95R_{Jup}$, supported by the $\eta_p=0.91$. Despite a number of much fainter companions, the level of blending is low in this field, strengthening the case for a planetary explanation in this case.

4.0.21 1SWASP J204745.08+103347.9

This is another case of a clear 'V'-shaped dip implying a stellar companion in spite of a low (~0.03 mag) amplitude in a lightcurve which shows no signs of ellipsoidal variation. The estimated companion radius of $1R_{Jup}$ is belied by a long transit duration ($\eta_p=1.47$). The likelihood of blending in this case points to a stellar binary.

4.0.22 1SWASP J205027.33+064022.9

This bright ($V\sim10.2$ mag) star displays a very shallow (9.6 mmag) but clear 'U'-shaped dip with an out of transit lightcurve that shows slight signs of ellipsoidal variation. The photometric precision is

such that the transits are immediately obvious in the unfolded data. This is a good candidate, with a prediction companion radius of $0.92R_{Jup}$ though the transits are slightly longer than expected (η_p = 1.43). The star has two nearby companions of similar magnitude, so we have flagged it 'B' for a potential blend.

4.0.23 1SWASP J205308.03+192152.7

The very low amplitude (0.0068 mag) transit signal is just visible over the noise in this otherwise flat lightcurve but appears to exhibit a flat-bottomed dip. The amplitude means that despite a host star radius of $1.24R_{\odot}$ the estimated companion radius is only $0.87R_{Jup}$, supported by an η_p=1.04. The 5 nearby stars means that contamination of the photometry cannot be ruled out without further observations.

4.0.24 1SWASP J210009.75+193107.1

This folded lightcurve displays a shallow but clear 'U'-shaped dip which can also been seen in the unfolded data. The periodogram exhibits a strong peak on the frequency 1/3.054875 although the period is close to an integer multiple of 1 day. The predicted radius implies a Jovian-sized companion, supported by an η_p of 0.71, but this object does suffer from blending.

4.0.25 1SWASP J210151.43+072326.7

At V=12.476 mag, this is one of our faintest candidates, and the lightcurve has a commensurate level of noise, but transit-like dips can be seen in the unfolded data also and no other variability is visible in the lightcurve. The estimated companion radius of $0.92R_{Jup}$ is supported by η_p=0.99. This star does have three nearby objects of similar brightness, and a much fainter object within $\sim4''$, so blending is a possibility here.

4.0.26 1SWASP J210318.01+080117.8

This lightcurve shows a clear transit dip with believable width, depth and period and although the intrinsic noise makes the true morphology unclear there is no sign of any other variability. The measured duration is a close match for that predicted, and the companion radius of $1.01R_{Jup}$ makes this a strong candidate. A single nearby star raises a possibility of blending.

4.0.27 1SWASP J210352.56+083258.9

While noisy, this lightcurve clearly exhibits a ~0.02 mag dip and is flat out of transit though the relatively long period (close to the $4\times$ multiple of the 1 day alias) results in a certain amount of 'clumping' of datapoints. The $1.61R_{Jup}$ companion radius is on the borderline for a planetary companion, but is supported by an η_p=0.95. Three nearby stars mean that the photometry for this object could be contaminated and that follow-up observations are necessary.

4.0.28 1SWASP J210909.05+184950.9

This bright ($V \sim9.9$ mag) object shows a remarkably smooth lightcurve out of transit, allowing HUNTSMAN to detect the very shallow (8.2 mmag), 'U'-shaped transit dip. Closer inspection however, reveals a marked ellipsoidal variation, flagging this object as a probable stellar binary. The host star is found to be of mid F-type

yet the predicted companion radius is only $1.07R_{Jup}$, supported with an η_p of 0.71. While this object is certainly the brightest in its field, it is likely that nearby, fainter stars will have affected the SW-N photometry. We encourage follow-up observations of this target.

4.0.29 1SWASP J210912.02+073843.3

This star was included despite a high S/N_{ellip}=12.508 because the folded lightcurve appeared fairly flat to visual inspection, and showed clear, flat bottomed transits with a duration of 2.28 hrs & δ=0.0213 mag appropriate for an exoplanet. The F-type host star implies a R_p=1.52R_{Jup} & η_p=0.89. Further inspection reveals the object to be severely blended, so the true eclipses will be deeper. As they are flat bottomed, the orbit must be edge-on. The companion could therefore be a low mass star or brown dwarf and higher resolution photometry is recommended.

4.0.30 1SWASP J211608.42+163220.3

The brief dip in this flat lightcurve appears to be 'V'-shaped, although intrinsic noise makes the morphology difficult to judge. The strong $\Delta\chi^2$ peak implies a credible period of 3.47 days. The estimated companion radius is Jovian at $1.18R_{Jup}$ though the low η_p of 0.59 implies the observed duration is shorter than predicted. As this star does not suffer from any blending it is a strong candidate for follow-up.

4.0.31 1SWASP J211645.22+192136.8

This object has a relatively long period of ~4.4 days which means that a single observing station will normally only observe roughly one transit in two, weather permitting. For this reason there are some gaps in the lightcurve and, although a reasonable number of transits were detected, there is a higher degree of uncertainty on the period. This may explain the somewhat unclear transit curve. Nevertheless, this is a promising candidate: it is an isolated bright object, and the predicted companion radius is $1.23R_{Jup}$ with η_p=0.71.

4.0.32 1SWASP J212532.55+082904.4

The transit signal is clearly visible in this slightly noisy lightcurve though the shape is not well defined. The companion radius is large but still within the planetary range at $1.58R_{Jup}$, backed up by an η_p=0.82. There are no other stars close by this object, so it too is a target for further observations.

4.0.33 1SWASP J212843.62+160806.2

The folded lightcurve clearly shows a shallow dip of ~0.02 mag with a believable period of 1.376 days. Closer inspection is needed to spot faint signs of a secondary eclipse and possible ellipsoidal variation (S/N_{ellip}=8.841). The target has three objects nearby though all are $\geqslant4$ mags fainter. The late spectral type, derived from IR colours, leads us to suggest that this could be a low-mass binary.

4.0.34 1SWASP J212855.03+075753.5

The faintness ($V\sim12.2$ mag) of this host star and the long period result in a low number of transits detected, and an under sampled, sharply 'V'-shaped signal in a noisy, but apparently flat, lightcurve. The nearby presence of a star of similar magnitude will also have

contributed to the photometric uncertainty. The colour indicates a late G-type host star with a companion of radius 1.35R$_{Jup}$, though the measured transit duration is shorter than expected for a planet (η_p=0.58).

Table 3. Candidate list after Stage 4. $N_{bri,faint}$ gives the number of USNO-B1.0 objects listed within $48''$ of the target that are brighter or <5 mag fainter respectively. Spectral types marked with an asterisk were estimated from the 2MASS $J - H$ index in cases where the $V_{SW} - K$ index was at the extremity of the range, and unreliable. Borderline candidates are marked with † and are listed for information.

Identifier 1SWASP...	Period (days)	Duration (hrs)	δ (mag)	$V_{SW} - K$	$J - H$	Spectral Type	R_* ($R_{\odot}$)	R_p (R_{Jup})	η_p	N_{bri}	N_{faint}	R	Codes Eta	Blend
†J175919.79+353935.1	4.846186	4.272	0.026	3.51	0.61	M0	0.64	0.88	1.58	0	2	A	C	B
†J180103.13+511557.1	4.785081	3.672	0.0145	2.46	0.48	K4	0.73	0.75	1.3	0	1	B	A	B
J180304.96+264805.4	2.364723	5.136	0.0254	2.52	0.53	K4	0.72	0.98	2.26	0	6	A	C	C
J180726.64+224227.9	4.246971	4.752	0.0205	1.91	0.29	G9	0.87	1.06	1.56	0	2	A	C	B
†J181129.19+235412.4	4.234895	8.568	0.0578	1.91	0.48	G9	0.87	1.78	2.61	0	2	C	C	B
J181317.03+305356.0	**2.248420**	**1.896**	**0.0145**	**1.6**	**0.28**	**G3**	**1.02**	**1.05**	**0.71**	**0**	**2**	**A**	**A**	**B**
J181454.99+391146.0	**1.102625**	**1.56**	**0.0235**	**2.89**	**0.74**	**K5**	**0.68**	**0.89**	**0.92**	**0**	**10**	**A**	**A**	**C**
J181958.25+492329.9	**2.368548**	**2.424**	**0.0061**	**1.57**	**0.26**	**G2**	**1.04**	**0.69**	**0.92**	**0**	**2**	**A**	**A**	**B**
J182127.09+200011.7	2.647752	4.248	0.0366	1.26	0.18	F7	1.25	2.04	1.27	0	6	C	A	C
J182131.07+483735.5	1.809191	2.832	0.0167	0.56	0.26	A7-F0	1.79	1.97	0.82	0	3	C	C	C
J182333.22+222801.2	1.821008	3.432	0.0421	1.59	0.21	G3	1.03	1.8	1.29	0	2	C	A	B
†J182339.64+210805.5	1.585846	2.088	0.0245	1.16	0.28	F6	1.32	1.76	0.74	0	13	C	A	C
J182346.12+434241.3	11.87746	6.841	0.065	1.26	0.19	F7	1.25	2.72	1.19	0	1	C	A	B
J182620.36+475902.8	**3.04365**	**4.032**	**0.0628**	**2.35**	**0.45**	**K3**	**0.75**	**1.6**	**1.49**	**0**	**0**	**B**	**A**	**A**
†J182626.38+374954.8	4.698312	4.944	0.0157	1.26	0.25	F7	1.25	1.34	1.29	0	6	A	A	C
J182916.00+235724.8	8.901122	4.168	0.038	1.48	0.34	G0	1.1	1.83	0.9	0	6	C	A	C
J182924.67+232200.2	**3.678186**	**2.952**	**0.0173**	**1.45**	**0.21**	**G0**	**1.12**	**1.26**	**0.88**	**0**	**3**	**A**	**A**	**C**
†J182927.04+233217.1	4.903747	4.704	0.0063	2.5	0.52	K4	0.73	0.49	1.71	0	5	A	C	C
†J183043.97+230526.1	3.680977	4.296	0.0098	1.68	0.26	G5	0.98	0.83	1.43	0	2	A	A	B
J183104.01+323942.7	**2.378781**	**1.776**	**0.0089**	**1.33**	**0.21**	**F8**	**1.2**	**0.97**	**0.61**	**0**	**2**	**A**	**A**	**B**
J183104.12+243739.3	0.746192	3.836	0.0197	1.47	0.23	G0	1.1	1.32	1.96	0	6	A	C	C
J183431.62+353941.4	**1.846796**	**2.28**	**0.0127**	**1.12**	**0.2**	**F5**	**1.35**	**1.3**	**0.78**	**0**	**3**	**A**	**A**	**C**
†J183517.51+390316.2	4.073428	5.16	0.012	2.71	0.49	K5	0.7	0.65	2	0	7	A	C	C
J183723.62+373721.9	3.300887	4.32	0.0251	2.69	0.51	K5	0.7	0.95	1.73	0	4	A	C	C
J183805.57+423432.3	**3.515957**	**4.104**	**0.0197**	**2.51**	**0.55**	**K4**	**0.72**	**0.86**	**1.6**	**0**	**4**	**A**	**C**	**C**
J184119.02+403008.4	**3.734014**	**4.224**	**0.0148**	**1.86**	**0.29**	**G8**	**0.89**	**0.92**	**1.45**	**0**	**1**	**A**	**A**	**B**
J184303.62+462656.4	**10.07384**	**7.253**	**0.037**	**2.3**	**0.55**	**K3**	**0.76**	**1.25**	**1.86**	**0**	**3**	**A**	**C**	**C**
J202820.25+094651.0	2.146933	4.776	0.0085	2.37	0.48	K3	0.75	0.59	2.23	0	2	A	C	B
J202824.02+192310.2	**1.257835**	**2.424**	**0.0222**	**1.2**	**0.2**	**F6**	**1.29**	**1.64**	**0.94**	**0**	**8**	**B**	**A**	**C**
†J202907.09+171631.7	4.117398	4.968	0.0309	1.61	0.37	G3	1.02	1.53	1.46	0	13	A	A	C
J203054.12+062546.4	**2.152102**	**1.296**	**0.0168**	**2.35**	**0.41**	**K3**	**0.75**	**0.83**	**0.59**	**0**	**3**	**A**	**A**	**C**
†J203229.10+132820.9	4.632829	4.608	0.047	2.35	0.61	K3	0.75	1.39	1.51	0	15	A	C	C
J203247.55+182805.3	2.522688	7.776	0.0118	1.42	0.27	F9	1.14	1.06	2.66	0	10	A	C	C
J203314.77+092823.4	**1.753056**	**3.048**	**0.0316**	**3.87**	**0.77**	**M0**	**0.62**	**0.94**	**1.59**	**0**	**2**	**A**	**C**	**B**
J203315.84+092854.2	**1.752371**	**2.784**	**0.0413**	**-0.46**	**0.198**	**F2-F5***	**1.46**	**2.53**	**0.87**	**1**	**12**	**C**	**A**	**C**
J203543.98+072641.1	1.85463	2.76	0.0195	0.99	0.24	F3	1.43	1.7	0.9	0	3	B	A	C
J203704.92+191525.1	**1.68011**	**1.416**	**0.0095**	**1.37**	**0.27**	**F9**	**1.17**	**0.97**	**0.55**	**0**	**2**	**A**	**A**	**B**
J203717.02+114253.5	3.118049	2.496	0.0274	1.31	0.25	F8	1.21	1.71	0.74	0	1	B	A	B
J203906.39+171345.9	**2.696631**	**2.184**	**0.0217**	**1.33**	**0.22**	**F8**	**1.2**	**1.35**	**0.79**	**0**	**2**	**A**	**A**	**B**
†J203932.30+162451.1	1.520504	8.976	0.02	3.35	0.62	K7	0.65	0.78	4.92	0	2	A	C	B
J204125.28+163911.8	**1.221506**	**2.88**	**0.008**	**2.77**	**0.54**	**K5**	**0.69**	**0.53**	**1.71**	**0**	**4**	**A**	**C**	**C**
†J204142.31+052007.5	3.216912	4.776	0.0279	2.05	0.38	K0	0.82	1.17	1.75	0	5	A	C	C
J204142.49+075051.5	**2.763125**	**2.328**	**0.0102**	**2.86**	**0.59**	**K5**	**0.69**	**0.59**	**1.04**	**0**	**4**	**A**	**A**	**C**

Table 3 – *continued* Candidate list after Stage 4. $N_{bri,faint}$ gives the number of USNO-B1.0 objects listed within 48″of the target that are brighter or <5 mag fainter, respectively. 1SWASP J211448.98+203557.1 was identified in two fields, SW2114+1628 & SW2115+2351 and independent results are given for each. Spectral types marked with an asterisk were estimated from the 2MASS $J − H$ index in cases where the $V_{SW} − K$ index was at the extremity of the range, and unreliable. Borderline candidates are marked with † and are listed for information. Parenthesis around an object indicates that spectroscopic data are discussed in Section 5.

Identifier 1SWASP...	Period (days)	Duration (hrs)	δ (mag)	$V_{SW} − K$	$J − H$	Spectral Type	R_* ($R_⊙$)	R_p (R_{Jup})	η_p	N_{bri}	N_{faint}	Code		
J204211.19+240145.1	3.362228	2.664	0.0544	1.65	0.19	G4	1.0	1.99	0.81	0	2	C	C	B
J204323.83+263818.7	**1.421123**	**1.32**	**0.0366**	**2.1**	**0.32**	**K1**	**0.81**	**1.32**	**0.63**	**0**	**2**	**A**	**A**	**B**
†J204328.95+054823.1	3.939179	2.328	0.0617	1.69	0.25	G5	0.97	2.06	0.68	0	2	C	A	B
(J204456.57+182136.0	8.147196	7.821	0.044	1.61	0.24	G3	1.02	1.83	1.79	0	2	C	C	B)
J204617.02+085412.0	**1.947141**	**2.184**	**0.0095**	**1.48**	**0.25**	**G0**	**1.1**	**0.91**	**0.84**	**0**	**5**	**A**	**A**	**C**
J204712.42+202544.5	**2.61264**	**2.064**	**0.0275**	**3.01**	**0.58**	**K5***	**0.67**	**0.95**	**0.91**	**0**	**8**	**A**	**A**	**C**
J204745.08+103347.9	**3.235407**	**3.648**	**0.0289**	**2.79**	**0.63**	**K7***	**0.69**	**1.00**	**1.47**	**0**	**2**	**A**	**A**	**B**
†J204905.55+110000.4	1.371571	1.584	0.023	1.07	0.24	F5	1.38	1.79	0.57	0	7	C	A	C
J205027.33+064022.9	**1.229345**	**3.192**	**0.0096**	**1.47**	**0.24**	**G0**	**1.1**	**0.92**	**1.43**	**0**	**2**	**A**	**A**	**B**
†J205218.75+182330.0	2.197814	3.48	0.0441	1.45	0.2	G0	1.12	2.01	1.17	0	4	C	A	C
J205223.03+151046.8	2.910170	2.400	0.0409	1.5	0.2	G1	1.08	1.86	0.75	0	0	C	A	A
J205302.40+201748.3	4.931719	8.88	0.0084	1.58	0.33	G2	1.03	0.81	2.61	0	1	A	C	B
J205308.03+192152.7	**1.676449**	**2.736**	**0.0068**	**1.27**	**0.21**	**F7**	**1.24**	**0.87**	**1.04**	**0**	**5**	**A**	**A**	**C**
J205438.05+105040.7	4.198031	3.048	0.0468	1.42	0.19	F9	1.14	2.10	0.81	0	0	C	A	A
J210009.75+193107.1	**3.054875**	**2.424**	**0.0082**	**1.08**	**0.11**	**F5**	**1.38**	**1.07**	**0.71**	**0**	**1**	**A**	**A**	**B**
†J210130.24+190021.7	2.683466	1.608	0.0709	1.9	0.34	G9	0.88	2	0.56	0	3	C	A	C
J210151.43+072326.7	**2.220785**	**2.472**	**0.0138**	**1.79**	**0.33**	**G7**	**0.92**	**0.92**	**0.99**	**0**	**3**	**A**	**A**	**C**
†J210231.79+101014.5	1.506187	1.608	0.0296	1.79	0.35	G7	0.92	1.35	0.71	0	6	A	A	C
J210318.01+080117.8	**1.223824**	**1.92**	**0.0167**	**1.79**	**0.31**	**G7**	**0.92**	**1.01**	**0.93**	**0**	**1**	**A**	**A**	**B**
†J210335.82+125637.6	1.447543	2.856	0.0146	1.27	0.18	F7	1.24	1.28	1.11	0	2	A	A	B
J210352.56+083258.9	**3.89368**	**3.504**	**0.0227**	**1.25**	**0.2**	**F7**	**1.25**	**1.61**	**0.95**	**0**	**3**	**B**	**A**	**C**
J210909.05+184950.9	**2.91879**	**2.664**	**0.0083**	**0.86**	**0.07**	**F1**	**1.51**	**1.17**	**0.75**	**0**	**3**	**A**	**A**	**C**
J210912.02+073843.3	**1.36983**	**2.28**	**0.0213**	**1.3**	**0.21**	**F8**	**1.22**	**1.52**	**0.89**	**0**	**2**	**A**	**A**	**B**
J211127.41+182653.3	4.216933	3.168	0.0464	1.44	0.19	G0	1.12	2.06	0.85	0	5	C	A	C
J211417.15+112741.0	6.579094	8.23	0.0336	1.6	0.35	G3	1.02	1.6	2.06	0	3	B	C	C
J211448.98+203557.1	4.864623	4.656	0.0530	1.63	0.25	G3	1.01	1.98	1.25	0	4	C	A	C
J211448.98+203557.1	4.864666	4.632	0.0525	1.63	0.25	G3	1.01	1.98	1.25	0	4	C	A	C
J211608.42+163220.3	**3.468244**	**1.992**	**0.0131**	**1.31**	**0.21**	**F8**	**1.21**	**1.18**	**0.59**	**0**	**0**	**A**	**A**	**A**
J211645.22+192136.8	**4.400381**	**2.640**	**0.0135**	**1.27**	**0.16**	**F7**	**1.24**	**1.23**	**0.71**	**0**	**0**	**A**	**A**	**A**
J211817.92+182659.9	7.715382	8.888	0.0357	1.04	0.3	F4	1.4	2.45	0.4	0	7	C	B	C
J212532.55+082904.4	**3.125014**	**2.688**	**0.0267**	**1.43**	**0.23**	**F9**	**1.13**	**1.58**	**0.82**	**0**	**0**	**A**	**A**	**A**
J212749.35+190246.0	7.810082	8.4	0.10	2.08	0.34	K1	0.82	2.21	2.05	0	1	C	C	B
†J212815.28+082933.7	4.91815	5.592	0.0083	1.27	0.23	F7	1.24	0.96	1.48	0	3	A	A	C
J212843.62+160806.2	**1.375647**	**2.64**	**0.0159**	**2.59**	**0.53**	**K5***	**0.71**	**0.76**	**1.44**	**0**	**3**	**A**	**A**	**C**
J212855.03+075753.5	**4.688048**	**1.92**	**0.0297**	**1.8**	**0.36**	**G7**	**0.92**	**1.35**	**0.58**	**0**	**2**	**A**	**A**	**B**
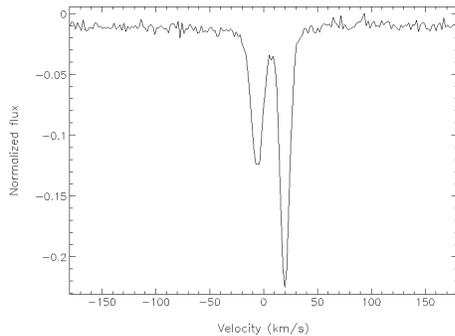
Figure 8. Deconvolved spectrum of 1SWASP J204456.57+182136.0 taken with ESPaDOnS at CFHT

5   SPECTROSCOPIC CONFIRMATION OF CANDIDATE ASSESSMENT

While the analysis discussed above was at a preliminary stage, the opportunity arose to obtain echelle spectra of 7 objects using the ESPaDOnS spectrograph on the Canada-France-Hawai'i Telescope, Hawai'i (CFHT) between 2005 September 23–24. These targets were taken from a preliminary selection list, according to the visibility from the telescope. The spectrograph was configured in spectropolarimetric mode during these observations, with a 79 rules/mm grating achieving a resolution of $R \sim 68,000$ and spanning over 40 orders in wavelength between 370–1050 nm. The filter in place was Stokes I band, and the exposure time was set between 300-600s, depending on the magnitude of the target. These data were reduced at the telescope using the *Libre-ESpRIT* [3] online data reduction facility to perform the usual bias subtraction, flat-fielding and wavelength calibrations, followed by the order extraction of the polarisation information.

Echelle spectroscopy provides a wavelength range of several thousand Angstroms and hence a large number (n_l=4688) of images of a large sample (3507) of photospheric lines. These were used to boost the signal-to-noise of the spectra by a factor of $\sim \sqrt{(n_l)}$ by applying the Least Squares Deconvolution method (see e.g. Donati & Collier Cameron 1997) in conjunction with a G2 line list. This analysis increased the S/N from $\sim$30 to $\sim$323. The telluric water lines within the echellogram were used to obtain a velocity calibration accurate to $\sim$few m/s of the heliocentric reference frame.

One of these stars, 1SWASP J204456.57+182136.0, falls within this dataset. This object survived the selection procedure as far as the final stage, where it received a grade of 'CCB' because of a high companion radius estimate ($1.83R_{Jup}$) and η_p=1.79. The low number of transits is a consequence of the long period ($\sim$8.15 days). Under our current selection procedure, this object was judged to be a blended stellar binary independently of the spectroscopic data. This assessment was confirmed by the CFHT spectra, shown in Figure 8, which clearly shows a double-lined binary. These data give us confidence that our candidate selection procedure eliminates many astrophysical false positives, and prioritises strong exoplanet candidates for follow-up observations.

[3] http://www.cfht.hawaii.edu/Instruments/Spectroscopy/Espadons/Espadons_esprit.html

Table 4. Priority exoplanet candidates.

Identifier 1SWASP...	Period (days)	Duration (hrs)	Depth (mag)	R_p (R_{Jup})
J183104.01+323942.7	2.378781	1.776	0.0089	0.97
J184119.02+403008.4	3.734014	4.224	0.0148	0.92
J204712.42+202544.5	2.61264	2.064	0.0275	0.95
J210318.01+080117.8	1.223824	1.92	0.0167	1.01
J211608.42+163220.3	3.468244	1.992	0.0131	1.18
J211645.22+192136.8	4.400381	2.640	0.0135	1.23

6   DISCUSSION

We have whittled down the original HUNTSMAN list of 11,626 stars observed between RA=18 hr–21 hr and have identified 35 objects of particular interest which we recommend for follow-up observations. We find 6 objects for which all the data currently at our disposal supports the hypothesis that the companion object is planetary. These are summarised in Table 4. However, we encourage investigation of all these objects, since some narrowly missed the priority list, chiefly due to blending. In the tabulated data and discussions above we have noted any causes of uncertainty on a case-by-case basis. Furthermore, 'false alarms' from transit surveys provide a new sample of low-mass binaries, which are of interest in their own right.

The SW-N instrument has proven to be an excellent way of finding transiting candidates among millions of bright field stars but it cannot conclusively determine the nature of these systems alone. As experience from a number of earlier transit surveys has shown (e.g. OGLE Udalski et al. 2004, Vulcan Borucki et al. 2001), a large ($\sim$90%) percentage of the candidates will turn out to be stellar binaries. Lister et al. (2006) estimate that $\sim$20–30 genuine exoplanets will be discovered in the 2004 season data as a whole, so we anticipate 2–4 to lie within this sample. This is an inescapable part of the nature of transit surveys: there are many astrophysical phenomena which mimic the signal of a transiting exoplanet (for a discussion, see Brown 2003, Charbonneau et al. 2004). Some of our candidates will be binary stars eclipsing at grazing incidence as seen from Earth, others are likely to be binaries whose eclipses appear shallower than they are in reality because of light from a third object contaminating our photometry.

It is therefore necessary to execute a systematic and careful series of follow-up observations to finally establish the true nature of these objects, and in the process, accurately determine their physical and orbital parameters. We have an extensive program of photometric and spectroscopic follow-up on-going. We initially obtain 1–2 medium-resolution spectra of all priority candidates to confirm the spectral typing and hence the estimate of the minimum companion radius. These data will also eliminate single- and double-lined binaries and line-of-sight blends from the asymmetries in the line profiles. An imaging campaign running in parallel provides high-precision two-colour photometry at higher resolution around the times of transit of the best candidates. This can identify stellar companions from a detectable ($\lesssim$0.01 mag) difference in transit depth. Finally, the best candidates are subject to full radial velocity observations.

Note: Shortly after this paper was submitted, our follow-up program confirmed the planetary nature of the companion to the shortlisted star 1SWASP J203054.12+062546.4, henceforth dubbed WASP-2b. For a detailed discussion of this discovery, see Cameron et al. (2007).

(a) 1SWASP J181317.03+305356.0

(b) 1SWASP J181454.99+391146.0

(c) 1SWASP J181958.25+492329.9

(d) 1SWASP J182620.36+475902.8

(e) 1SWASP J182924.67+232200.2

(f) 1SWASP J183104.01+323942.7

(g) 1SWASP J183431.62+353941.4

(h) 1SWASP J183805.57+423432.3
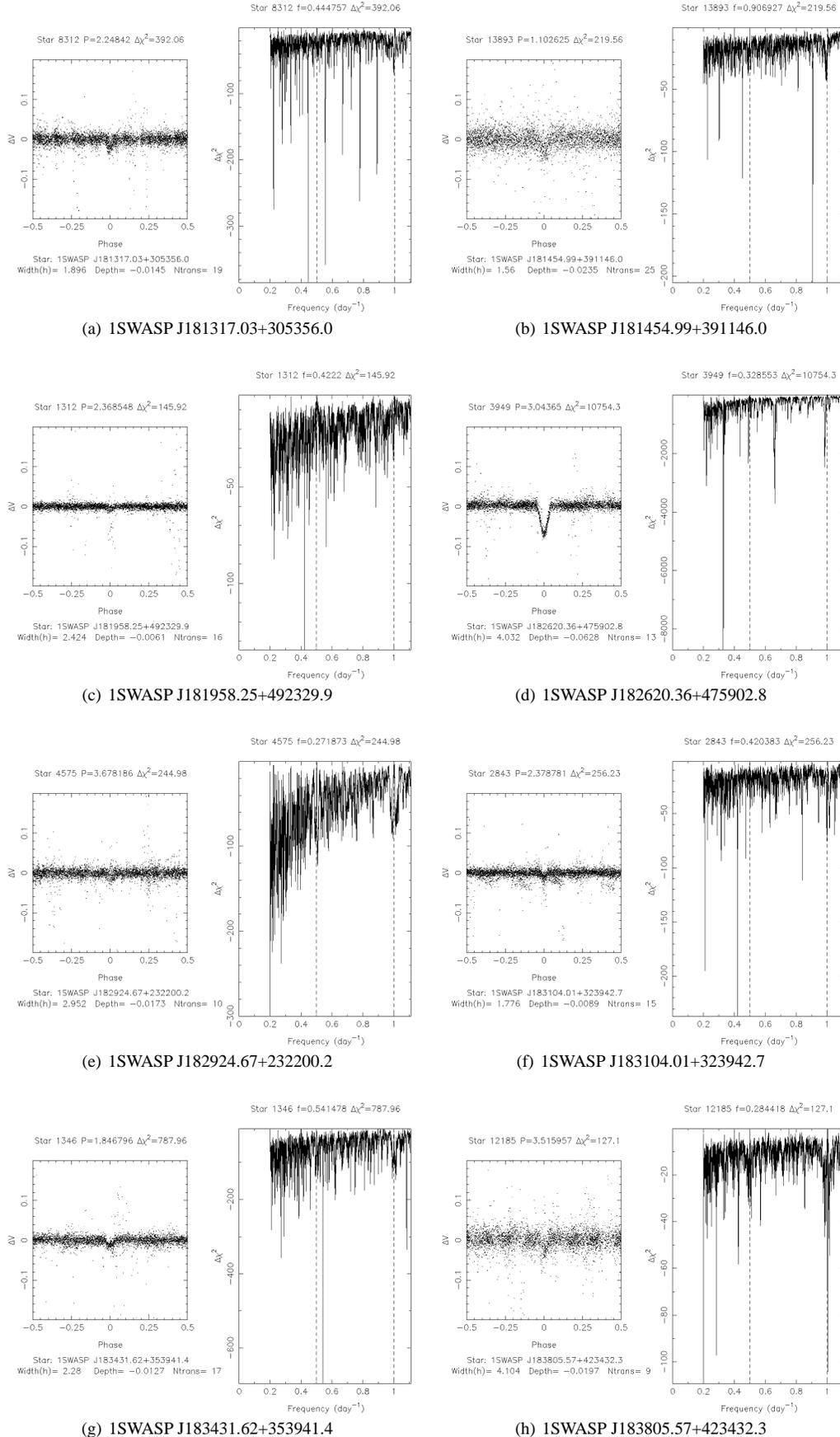
Figure 3. The lightcurves of the selected transit candidates, folded on the measured period.

(a) 1SWASP J184119.02+403008.4

(b) 1SWASP J184303.62+462656.4

(c) 1SWASP J202824.02+192310.2

(d) 1SWASP J203054.12+062546.4

(e) 1SWASP J203314.77+092823.4

(f) 1SWASP J203315.84+092854.2

(g) 1SWASP J203704.92+191525.1

(h) 1SWASP J203906.39+171345.9
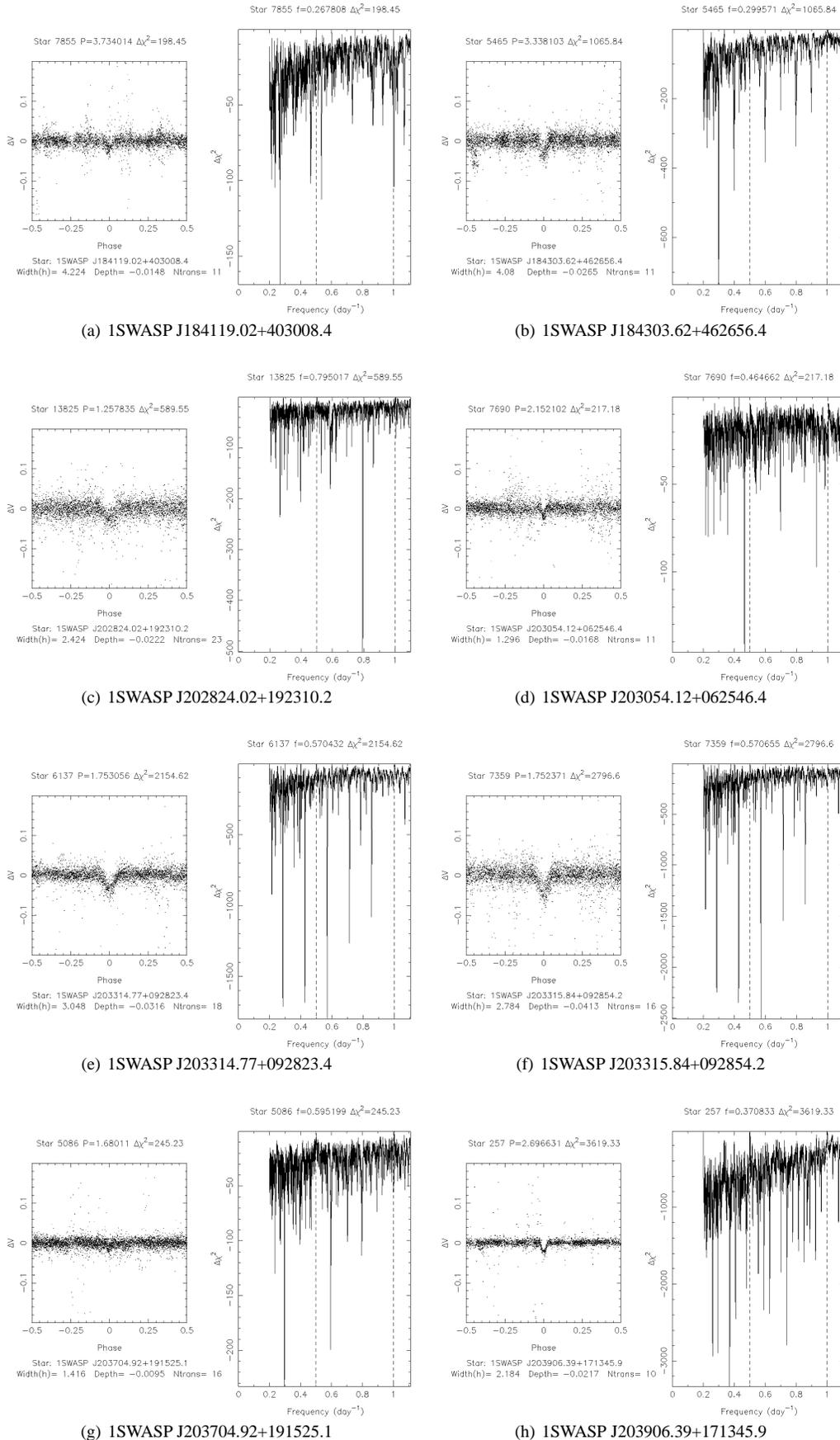
Figure 4. The lightcurves of the selected transit candidates, folded on the measured period.

(a) 1SWASP J204125.28+163911.8

(b) 1SWASP J204142.49+075051.5

(c) 1SWASP J204323.83+263818.7

(d) 1SWASP J204617.02+085412.0

(e) 1SWASP J204712.42+202544.5

(f) 1SWASP J204745.08+103347.9

(g) 1SWASP J205027.33+064022.9

(h) 1SWASP J205308.03+192152.7
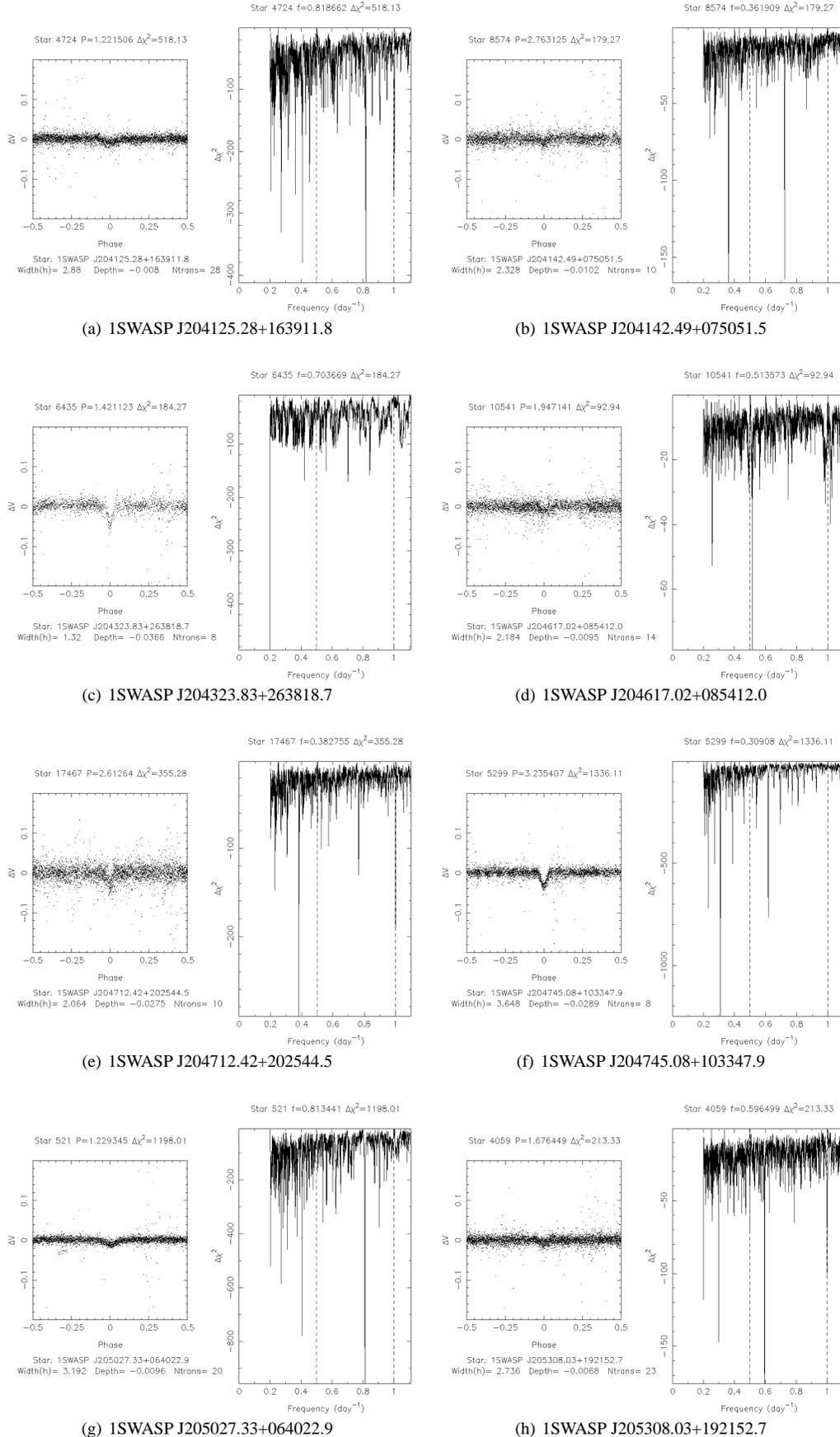
Figure 5. The lightcurves of the selected transit candidates, folded on the measured period.

(a) 1SWASP J210009.75+193107.1

(b) 1SWASP J210151.43+072326.7

(c) 1SWASP J210318.01+080117.8

(d) 1SWASP J210352.56+083258.9

(e) 1SWASP J210909.05+184950.9

(f) 1SWASP J210912.02+073843.3

(g) 1SWASP J211608.42+163220.3

(h) 1SWASP J211645.22+192136.8
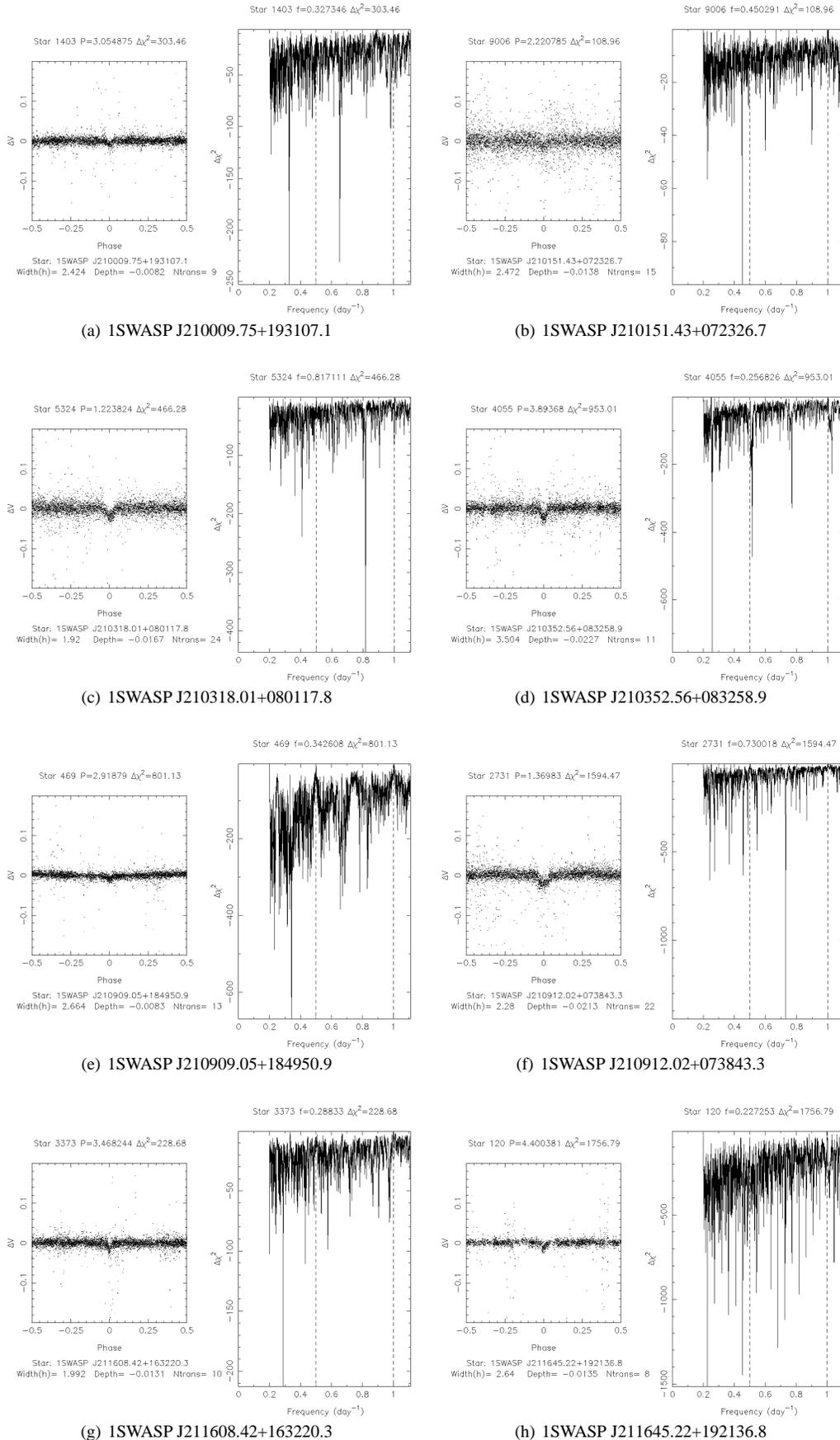
Figure 6. The lightcurves of the selected transit candidates, folded on the measured period.

(a) 1SWASP J212532.55+082904.4

(b) 1SWASP J212843.62+160806.2

(c) 1SWASP J212855.03+075753.5
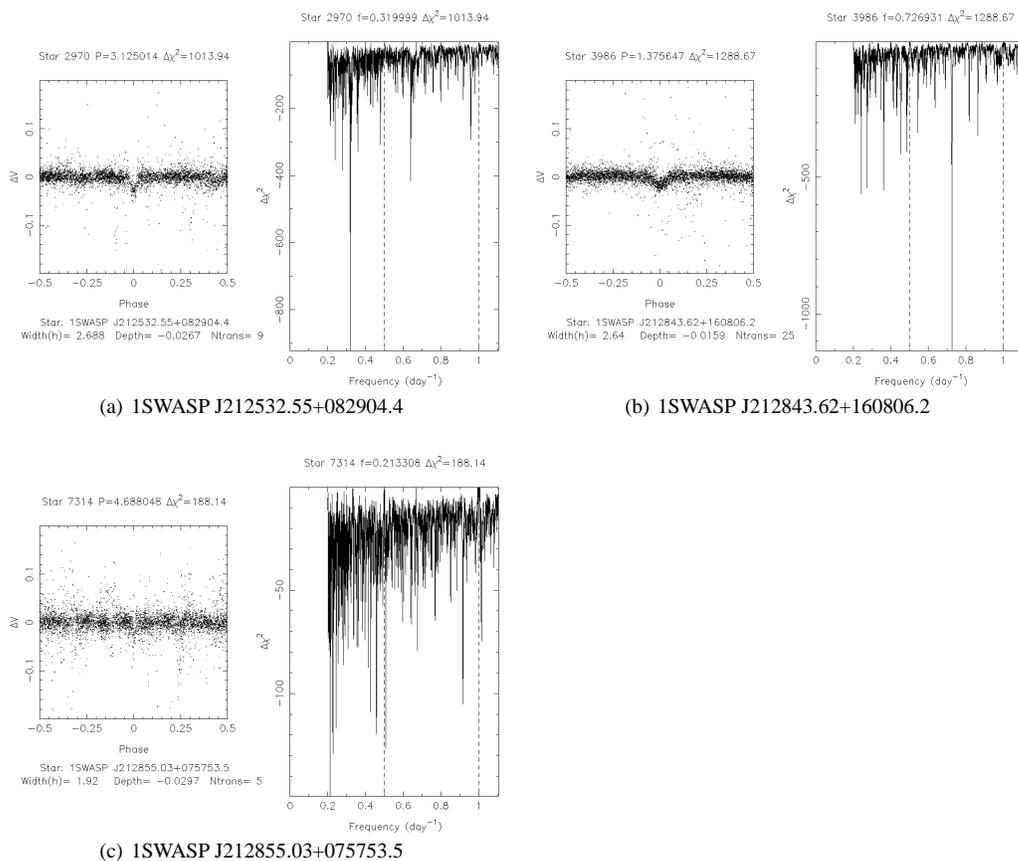
Figure 7. The lightcurves of the selected transit candidates, folded on the measured period.

7 ACKNOWLEDGEMENTS

REFERENCES

Ammons S., Robinson S., Strader J., Laughlin G., Fischer D., Wolf A., 2006, ApJ, 638, 1004

Borucki W. J., Caldwell D., Koch D. G., Webster L. D., Jenkins J. M., Ninkov Z., Showen R., 2001, PASP, 113, 439

Brown T., 2003, ApJ, 593, L125

Brown T. M., Charbonneau D., Gilliland R. L., Noyes R. W., Burrows A., 2001, ApJ, 552, 699

Burke C., Gaudi B., DePoy D., Pogge R., 2006, AJ, 130, 210

Burrows A., Guillot T., Hubbard W. B., Marley M. S., Saumon D., Lunine J. I., Sudarsky D., 2000, ApJ, 534, L97

Cabanela J., Humphreys R., Aldering G., Larsen J., Odewahn S., Thurmes P., Cornuelle C., 2003, PASP, 115, 837

Cameron A. C., Bouchy F., Hébrard G., Maxted P., Pollacco D., Pont F., Skillen I., Smalley B., Street R. A., West R. G., Wilson D. M., Aigrain S., Christian D. J., Clarkson W. I., 25 others 2007, MNRAS, 375, 951

Chabrier G., T. B., Baraffe I., Allard F., Hauschildt P., 2004, ApJ, 603, L53

Charbonneau D., Brown T., Burrows A., Laughlin G., 2007, in Protostars and Planets V University of Arizona Press, pp 701–716

Charbonneau D., Brown T., Dunham E., Latham D., Looper D., Mandushev G., 2004, in The Search for Other Worlds: Fourteenth Astrophysics Conference AIP Conference Proceedings, pp 151–160

Charbonneau D., Brown T., Noyes R., Gilliland R., 2002, ApJ, 568, 377

Christian D., Pollacco D., Skillen I., Street R., Keenan F., Clarkson W., Collier Cameron A., Kane S., Lister T., West R., Enoch R., Evans A., Fitzsimmons A., Haswell C., 10 others 2006, MNRAS, 372, 1117

Collier Cameron A., Pollacco D., Street R. A., Lister T. A., West R. G., Wilson D. M., Pont F., Christian D. J., Clarkson W. I., Enoch B., Evans A., Fitzsimmons A., Haswell C. A., Hellier C., 11 others 2006, MNRAS, 373, 799

Cox A., 2000, Allen's Astrophysical Quanities. Springer, 4th Ed.

Donati J.-F., Collier Cameron A., 1997, MNRAS, 219, 1

Gray D. F., 1992, The observation and analysis of stellar photospheres, 2nd edition. CUP, University of Cambridge

Høg E., Fabricius C., Makarov V. V., Urban S., Corbin T., Wycoff G., Bastian U., Schwekendiek P., Wicenec A., 2000, A&A, 355, L27

Ipatov S., 1993, Astronomicheskii Vestnik, 27, 83

Lin D. N. C., Bodenheimer P., Richardson D. C., 1996, Nat, 380, 606

Lister T., West R., Wilson D., Collier Cameron A., Clarkson W., Street R., Enoch R., Parley N., Christian D., Kane S., Evans A., Fitzsimmons A., Haswell C., Hellier C., 10 others 2006, MNRAS

O'Donovan F., Charbonneau D., Torres G., Mandushev G., Dunham E., Latham D., Alonso R., Brown T., Esquerdo G., Everett M., Creevey O., 2006, ApJ

Perryman M., Lindegren L., Kovalevsky J., Hoeg E., Bastian U., Bernacca P., Crézé M., Donati F., Grenon M., van Leeuwen F., van der Marel H., Mignard F., Murray C. A., Le Poole R., Schrijver H., Turon C., Arenou F., Froeschlé M., Petersen C., 1997, A&A, 323, L49

Pollacco D., Skillen I., Cameron A., Christian D., Irwin J., Lister T., Street R., West R., Clarkson W., Deeg H., Evans A., Fitzsimmons A., Haswell C., Hellier C., Hodgkin S., Horne K., Jones B.,

Kane S., Keenan F., Norton A., Osborne J., Ryans R., Wheatley P., 2006, A&A

Pont F., Zucker S., Queloz D., 2006, MNRAS

Schwarzenberg-Czerny A., 1989, MNRAS, 241, 153

Schwarzenberg-Czerny A., 1999, ApJ, 516, 315

Skrutskie M. F., Cutri R. M., Stiening R., Weinberg M. D., Schneider S., Carpenter J. M., Beichman C., Capps R., Chester T., Elias J., Huchra J., Liebert J., Lonsdale C., Monet D. G., Price S., Seitzer P., Jarrett T., Kirkpatrick J. D. e., 2006, AJ, 131, 1163

Smith A. M. S., Collier Cameron A., Christian D. J., Clarkson W. I., Enoch B., Evans A., Haswell C. A., Hellier C., Horne K., Irwin J., Kane S. R., Lister T. A., Norton A. J., Parley N., 8 others 2006, MNRAS, 373, 1151

Steffen J., Agol E., 2005, MNRAS, 364, L96

Tingley B., Sackett P., 2005, ApJ, 627, 1011

Udalski A., Szymanski M., Kubiak M., Pietrzynski G., Soszynski I., Zebrun K., Szewczyk O., Wyrzykowski L., 2004, Acta Astron., 54, 313

Vidal-Madjar A., Désert J.-M., Lecavelier des Etangs A., Hébrard G., Ballester G., Ehrenreich D., Ferlet R., McConnell J., Mayor M., Parkinson C., 2004, ApJ, 604, L69

Vidal-Madjar A., Lecavelier des Etangs A., Désert J.-M., Ballester G., Ferlet R., Hébrard G., Mayor M., 2003, Nat, 422, 143

Wenger M., Ochsenbein F., Egret D., Dubois P., Bonnarel F., Borde S., Genova F., Jasniewicz G., Laloë S., Lesteven S., Monier R., 2000, A&AS, 143, 9

Wilson D., Christian D., Clarkson W., 32 others 2007, in Proceedings of the Transiting Extrasolar Planets Workshop ASP Conference Series

This paper has been typeset from a TeX/ LaTeX file prepared by the author.